wire-injured arteries. Our results show that only 3-day treatment with Epo causes mobilization of circulating $CD45^{dim}$/Flk-1^+ or $Sca1^+$/Flk-1^+ EPCs and stimulates both differentiation of BM-derived EPCs on the endothelial layer and proliferation of resident ECs associated with endothelial EpoR-mediated activation of the Akt-eNOS pathway and SMC antiapoptotic effect, resulting in a marked inhibition of neointimal formation.

Materials and Methods

Vascular Injury, Epo Administration, and Morphometric Analysis

Transluminal arterial injury was performed in 8-week-old male C57BL/6 mice. A straight spring wire (0.25 mm in diameter) was inserted into the left femoral artery and placed there for 3 minutes. This wire injury was reported to cause a complete removal of endothelium.[19] Human Epo (Chugai, Tokyo) (1000 IU/kg body weight) or saline was injected intraperitoneally just after arterial injury and once daily for the following 2 days. Treatment with N^G-nitro-L-arginine methyl ester (L-NAME) (3.7 mmol/L) or 2.25% L-arginine hydrochloride (106.8 mmol/L; Sigma) in the drinking water took place for 7 days before wire injury and continued for 14 days after wire injury.

The dose of Epo was determined based on the previous report.[13] The injured arteries were harvested at day 14 and fixed with 4% paraformaldehyde. Paraffin-embedded sections were stained with Elastica van Gieson. Three sections from each artery at 300-μm intervals were analyzed using ImageJ 1.32j software (NIH). In other animals, Evans blue dye (5%; Sigma) was transfused to mice 10 minutes before euthanasia to identify the remaining denuded area 5 and 14 days after wire injury. After removal, arterial tissues were longitudinally opened and then placed on slide glasses to take pictures under microscope (MS5 Olympus). All animal procedures were approved by institutional guidelines. The collection of blood samples and the consent protocol for the volunters was approved by institutional guidelines.

Fluorescence-Activated Cell Sorting

PB (100 μL) was collected 3 days after injury and incubated for 15 minutes with anti-mouse CD34–fluorescein isothiocyanate (FITC), Flk-1-PE, Sca1-FITC, CD45-PECy5 antibodies (BD Pharmingen). After erythrocyte lysis, cells were analyzed with FACS Caliber (Becton Dickinson). $CD45^{dim}$/Flk-1^+ cells and $Sca1^+$/Flk-1^+ cells were sorted with FACS Vantage to give a culture assay and RT-PCR analysis, respectively.

Murine Cell Culture Assay

The sorted $CD45^{dim}$/Flk-1^+ cells were cultured with EBM-2 medium supplemented with 5% FBS, EGM-2-MV-SingleQuots (Clonetics), and 10 ng/mL VEGF (Peprotech) on fibronectin-coated chamber slides (Becton Dickinson). Adherent cells were reseeded after 4 days and maintained for 7 days. The culture cells were incubated with 2.4 μL/mL Alexa Fluor 594-labeled acetylated LDL (acLDL) (Molecular Probes) for 120 minutes, fixed with 2% paraformaldehyde, and incubated with 10 ng/mL of BS-1-FITC (Sigma) for 1 hour, and double-fluorescent cells were counted as EPCs in 4 randomly selected fields under confocal microscopy (FLUOVIEW BX50; Olympus).

Immunohistochemistry

Arteries were harvested on day 14 and fixed in 4% paraformaldehyde. Paraffin cross-sections were stained with antibodies against CD31 (sc-8306; Santa Cruz Biotechnology) and EpoR (sc-5624 or sc-697) followed by the avidin–biotin complex technique and diaminobenzidine substrate (Vector Laboratories). Sections were counterstained with hematoxylin. Frozen sections were stained with antibodies (GFP-Alexa Fluor 488, Molecular Probes; CD31-PE, BD Pharmingen), followed by Alexa Fluor 633–conjugated anti-rabbit IgG secondary antibody (Molecular Probes), and then observed under the confocal microscopy. The number of fluorescent cells from 6 sections was evaluated statistically.

To detect apoptotic cells in situ, TdT-mediated dUTP-biotin nick end labeling (TUNEL) staining was performed for paraffin sections using the In-Situ Cell Death Detection Kit (Chemicon International Inc) and counterstained with methyl green.

BM Transplantation

GFP transgenic mice were generously provided from Dr Okabe (Osaka University).[20] ROSA mice[21] were purchased from The Jackson Laboratory (Bar Harbor, Me). GFP- or β-galactosidase–overexpressing BM cells (5×10^6) were transfused to recipient mice 24 hours after 9 Gray irradiation. Six weeks after transplantation, they were subjected to vascular injury. Subsequently, at day 14 after injury, mice were examined.

Human Cell Isolation and Culture

PB was obtained. PB MNCs from venous blood of healthy human volunteers were isolated by density-gradient centrifugation (Lymphoprep; Axis Shield). $CD133^+$ progenitor cells were purified from PB MNCs by positive selection with anti-$CD133^+$ microbeads respectively using magnetic cell sorter device (Miltenyi Biotec). The purity of sorted cells assessed by fluorescence-activated cell sorter (FACS) analysis was grater than 90%. The $CD133^+$ progenitor cells were cultured in EBM-2 medium supplemented with 5% FBS, EGM-2-MV-SingleQuots (Clonetics) a day before analysis, as described below. All cells were maintained at 37°C in a humidified incubator at 5% CO_2. After serum starved in DMEM supplemented with 0.5% FBS for 12 hours, they were stimulated with 1.2IU/mL of Epo for 30 minutes and fixed. Immunofluorescence was performed by using antibodies against EpoR (sc-5624; Santa Cruz Biotechnology) with phosphorylated Akt and eNOS (Cell Signaling Technology). For double staining, we used Zenon rabbit IgG labeling kits (Molecular Probes) only when needed.

For measurement of the intracellular NO level, the cells were loaded with 4-amino-5-methylamino-2′,7′-difluorofluorescein diacetate (DAF-FM DA) (10 μmol/L; Daiichi Pure Chemicals, Tokyo, Japan) for 30 minutes at 37°C in the dark, washed twice with buffer, incubated for another 30 minutes, and then visualized under laser microscopy.

Fluorescent intensity was evaluated with Adobe Photoshop software.

Measurement of NOx Concentration

NOx concentration in the serum was measured with a high-performance liquid chromatography (HPLC) Griess system, as previously described.[22]

Statistics

Statistical analyses were performed with 1-way ANOVA followed by pair-wise contrasts using the Dunnett's test. Data are expressed as means±SE for continuous variables. $P<0.05$ was considered statistically significant.

Results

Epo Inhibits Neointimal Hyperplasia

A prominent, concentric neointima developed in the saline-treated vessels 14 days after injury, whereas neointimal formation was markedly reduced in the Epo-treated animals (Figure 1A). Morphometric analysis of serial sections (Figure 1B) showed a marked decrease (52%, n=10, $P<0.05$) in the neointimal area in the Epo-treated mice compared with the saline-injected group. The ratio of intima to medial area (I/M ratio) in the Epo-treated mice was significantly smaller (46%, n=10, $P<0.05$) than that in the saline-treated mice, whereas

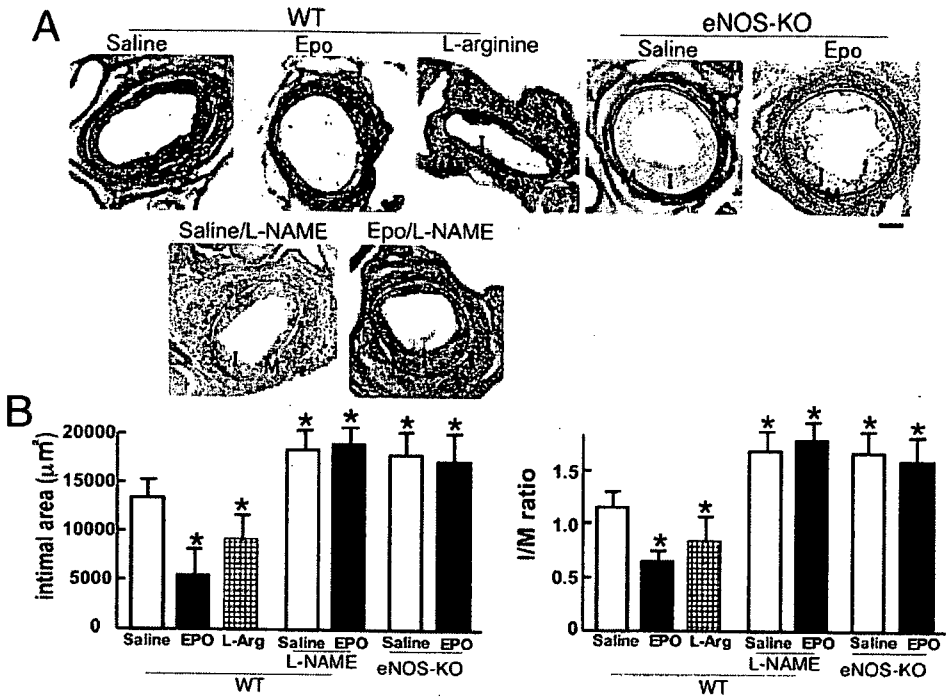

Figure 1. Epo-mediated inhibition of neointimal hyperplasia in NO-dependent manner. The wild-type or eNOS-null mice were subjected to the wire injury of femoral arteries and then treated with Epo or saline for the initial 3 days. Treatment with L-NAME (3.7 mmol/L) or 2.25% L-arginine hydrochloride (106.8 mmol/L) in the drinking water was started 7 days before wire injury and continued for 14 days until arterial sampling. A, Elastica van Gieson–stained sections on day 14. Scale bar=100 μm. I indicates intima; M, media. B, Quantification of the neointimal area and the I/M ratio averaged on 3 different sections of each artery (n=10 each). *$P<0.05$ vs saline-treated wild-type mice.

medial thickness did not significantly differ between either group (data not shown).

As the involvement of NO in the neointimal hyperplasia has been reported,[23] we next examined the effect of L-NAME on the Epo-mediated inhibition. Seven-day pretreatment with L-NAME significantly aggravated the neointimal hyperplasia in the saline-treated control mice (31%, n=10, $P<0.05$), consistent with the previous reports using eNOS-null mice.[24] Interestingly, L-NAME completely abolished Epo-mediated inhibitory effect on the neointimal hyperplasia (I/M ratio;1.61±0.38 versus 0.63±0.15 in the Epo-treat mice, $P<0.05$, n=10 each) (Figure 1A and 1B), suggesting the involvement of NO in Epo-mediated action. Furthermore, treatment with the NO donor L-arginine reduced the neointimal area to the level comparable to the Epo-treated mice (Figure 1A and 1B).

To confirm that the Epo-mediated inhibition of the neointimal formation is eNOS/NO dependent, we performed the arterial injury in the eNOS-null mice. The neointimal formation in the Epo-treated eNOS-null mice was aggravated (2.8-fold, n=7, $P<0.005$) compared with that of the Epo-treated wild-type mice, which was similar to the level in the Epo plus L-NAME–treated mice (2.9-fold, n=10, $P<0.005$) (Figure 1A and 1B).

The hemoglobin value was significantly higher after Epo treatment than that of the saline-treated controls (12.6±0.4 versus 14.0±0.1 g/dL at day 9, n=15, $P<0.05$). The number of white blood cells reached a peak on day 2 in both groups and was significantly higher in the Epo-treated mice (18 600±2020 versus 10 200±1100 cells/μL of control, n=15, $P<0.05$). The platelet number was similar in both groups on days 2 and 9.

Epo Promotes Reendothelialization

Evans blue dye was administered premortem to stain the nonendothelialized areas 5 and 14 days after injury. Nonendothelialized lesions are marked by blue staining, whereas the reendothelialized area appears white (Figure 2A). At both time points, the reendothelialized area in the Epo-treated group was significantly larger than that in the saline-treated group (1.4- and 1.8-fold on day 5 and -14, n=6, respectively) (Figure 2A). Immunostaining with anti-CD31 antibody in transverse sections revealed that the proportion of $CD31^+$ length to total lumen surface was 1.4-fold greater in the Epo-treated mice (n=10, $P<0.05$) (Figure 2B), consistent with the result from Evans Blue dye experiment. Furthermore, the NO dependency of the Epo-promoted reendothelialization was evaluated. The $CD31^+$ endothelial area in the total lumen length in the Epo plus L-NAME–treated mice was 65% lower than that in the Epo-treated mice (n=10, $P<0.01$) and similar to the saline-treated control mice (Figure 2B).

Epo Facilitates Mobilization of EPCs

$CD45^{dim}$ cells were gated from PB MNCs and subsequently analyzed for the expression of endothelial lineage markers, Flk-1 and CD34. Three-day Epo treatment mobilized the $CD45^{dim}$ cells into circulation (Figure 3A), and the ratio of $CD45^{dim}$/Flk-1^+ cells to total PB MNCs increased to 7.4-fold (n=5 each, $P<0.05$) (Figure 3A, right). We further investi-

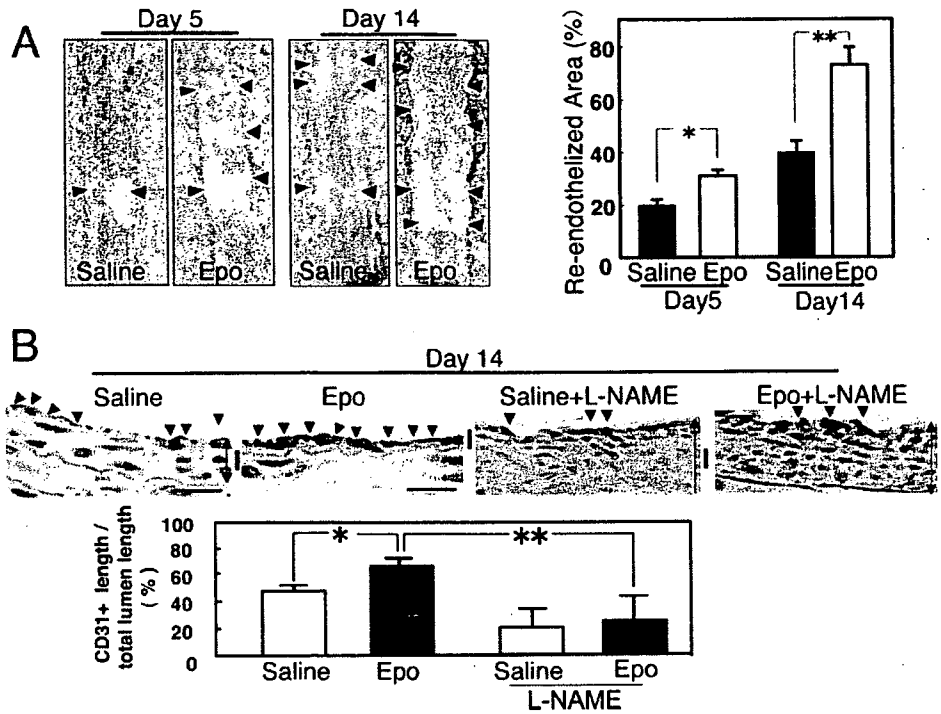

Figure 2. Epo facilitated reendothelialization after wire injury. A, Evans blue dye was injected 10 minutes before euthanasia on days 5 and 14. Nonendothelialized lesions are marked by blue staining, whereas the reendothelialized area appears white (arrowhead). Quantification of the reendothelialized areas was performed with computed morphometry (n=6 each, $^{*}P<0.01$, $^{**}P=0.02$). B, Fourteen days after arterial injury with and without L-NAME pretreatment, the lesion was subjected to histological analysis. ECs were identified by immunostaining with anti-CD31 antibody in day-14 artery samples. Apparent $CD31^{+}$ area is indicated by arrowheads. The ratio of $CD31^{+}$ length to lumen perimeter in sections were evaluated and averaged on 5 different cross-sections from each artery (n=10, $^{*}P<0.05$, $^{**}P<0.01$). I indicates intima.

gated the effect of L-NAME pretreatment on the Epo-mediated mobilization of EPCs using anti-Sca1 and anti-Flk-1 antibodies. The number of circulating $Sca1^{+}/Flk\text{-}1^{+}$ cells in the control group was markedly increased than the basal level (2-fold, n=6, $P<0.05$), whereas in the L-NAME–treated group, the Epo-mediated mobilization was completely inhibited (Figure 3B).

To confirm the endothelial property of $CD45^{dim}/Flk\text{-}1^{+}$ cells, we cultured them for 7 days in EGM medium with 10 ng/mL VEGF, and the EC-specific function was examined. Confocal microscopy demonstrated that 93±5% of cultured $CD45^{dim}/Flk\text{-}1^{+}$ cells were bound to FITC-conjugated BS-1 lectin and incorporated DiI-labeled acLDL, a commonly used identifier of endothelial lineage cells (Figure 3C). To evaluate the number of circulating EPCs, PB MNCs were isolated 3 days after Epo or saline treatment and cultured for 7 days. The relative numbers of BS-1 $lectin^{+}/acLDL^{+}$ cells from Epo-treated mice were 5.2±0.5-fold higher (n=5, $P<0.02$) than that in the saline-injected control (Figure 3D).

Antiapoptotic Effect on Medial SMC After Vascular Wire Injury

The procedure of wire injury of mouse femoral artery causes complete removal of endothelium, resulting in rapid apoptosis of medial SMCs that enhances neointimal hyperplasia.[19,25] Inhibition of this burst apoptosis is reported to be a preventive effect on neointimal hyperplasia.[26] Figure 3E shows that at 2 and 4 hours after injury, the number of TUNEL-positive apoptotic cells in the Epo-treated artery was significantly ($P<0.05$) decreased to 25% and 39% of the saline-treated controls, respectively. L-NAME treatment did not affect the Epo-mediated protection of VSMC apoptosis. Considering that the endothelium was completely removed by wire injury and the expression of EpoR in the EC-denuded artery was detected by RT-PCR analysis (unpublished observation, 2006), these findings suggest that Epo directly affects the apoptosis of VSMCs after wire injury. Interestingly, at 6 hours after injury, the number of apoptotic cell in the Epo-treated mice was increased to the level similar to the saline-treated mice, suggesting that Epo treatment did not prevent, but shifted, the apoptosis of VSMCs after wire injury.

The biological effects of Epo in the injured artery may be attributable to Epo-induced increase in circulating NO pool produced by the remote endothelial cells. Plasma NOx concentrations at 1, 2, 4, and 6 hours and 1, 3, and 14 days after injury of the Epo-treated mice were similar to those of the control mice (day 1: 54.3±8.6 versus 57.2±9.7; day 3: 58.6±9.6 versus 55.3±10.2; day 14: 59.6±4.6 versus 60.8±6.5 μmol/L; n=7 each). The expression levels for eNOS and EpoR in the lung and carotid artery at the same time points were comparable with the control mice when assessed by Western blotting and RT-PCR analysis, respectively (data not shown). These findings suggest that Epo-

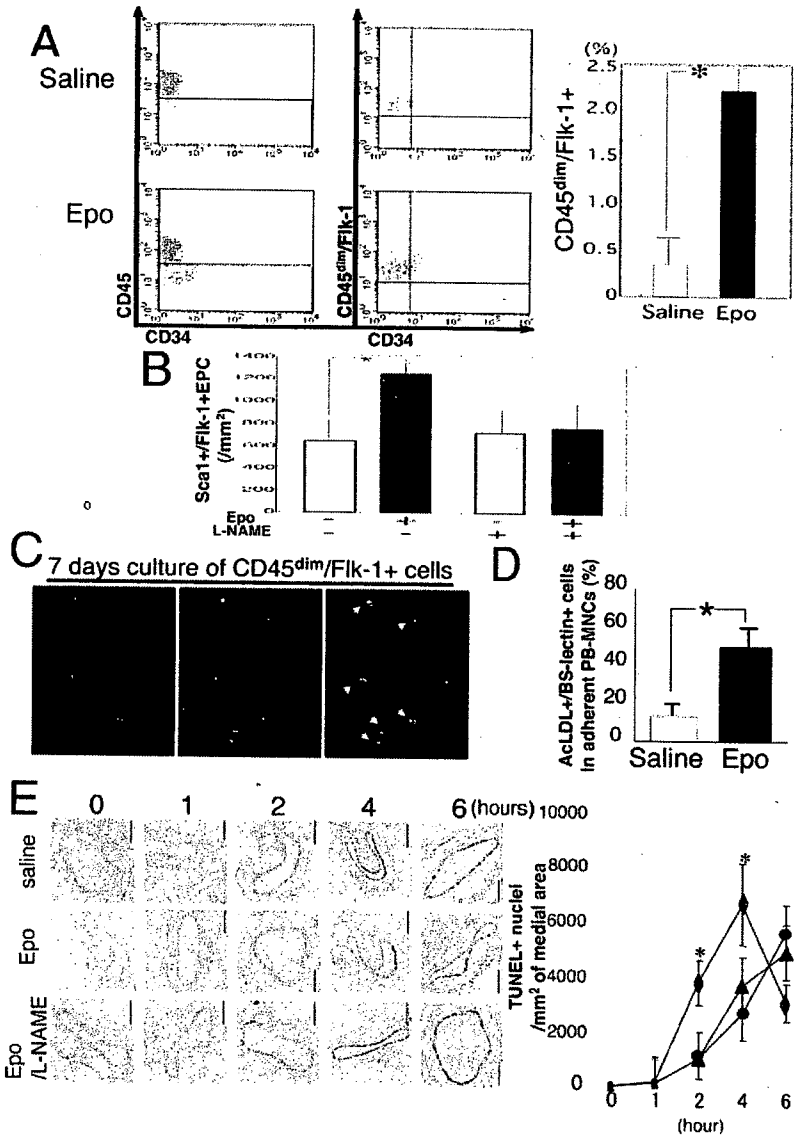

Figure 3. Identification of Epo-mobilized endothelial progenitor cells and antiapoptotic effect on medial SMCs. A, PB was collected 3 days after injury and subjected to FACS analysis. $CD45^{dim}$ cells were gated and subsequently analyzed for Flk-1 and CD34 expression. Right, Percentage of the $CD45^{dim}/Flk\text{-}1^+$ cells in total PB MNCs was higher in the Epo-treated group (n=5, $^*P<0.05$). B, Evaluation of the number of circulating $Sca1^+/Flk\text{-}1^+$ EPCs by FACS analysis. After 3 days of Epo treatment, the number of the circulating $Sca1^+/Flk\text{-}1^+$ EPCs per millimeter squared of PB of the mice with or without 7 days of L-NAME pretreatment was evaluated ($^*P<0.05$, each n=4). C, Differentiation of $CD45^{dim}/Flk\text{-}1^+$ cells into endothelial-lineage cells. PB MNCs were prepared from the 3-day Epo-treated mice, $CD45^{dim}/Flk\text{-}1^+$ cells were sorted and primarily cultured for 7 days, and the endothelial properties were examined by the uptake of DiI-acLDL and binding to FITC–BS-1 lectin. Cells in the merged image (right, arrowheads) indicate BS-1 $lectin^+/acLDL^+$ double-fluorescent cells. D, Total PB MNCs were primary cultured in endothelial medium for 7 days. The ratio of adherent cells with BS-1 $lectin^+/acLDL^+$ EC-like property was shown (n=5, $^*P<0.02$). E, Time course of the apoptosis in the injured artery. Femoral arteries of mice treated with Epo, Epo plus L-NAME, or saline (n=5 each) were analyzed before and after 1, 2, 4, and 6 hours after wire injury. Apoptotic nuclei were detected as brown dots by TUNEL staining. Right, Semiquantification of $TUNEL^+$ nuclei in the medial area. Diamond, circle, and triangle indicate saline-, Epo-, and Epo plus L-NAME–treated mice, respectively. $^*P<0.05$ vs to Epo- and Epo plus L-NAME–treated mice.

mediated action unlikely results from the nonspecific increase in circulating NO pool.

Analysis by BM Replacement Model

We further examined whether Epo actually induces the incorporation of marrow-derived EPCs into the regenerated endothelium by transplanting GFP-overexpressing or β-galactosidase BM cells to the BM-ablated background mice. Six weeks after transplantation, 96±2% and 94±3% of PB MNCs were replaced, respectively (n=5 each; FACS data not shown). The mice that received vascular injury were examined on day 14. GFP^+ and $\beta\text{-}Gal^+$ cells were patchily detected in the endothelial layer, and double-fluorescence immunohistochemistry (Figure 4A and 4B) disclosed a significant increase in the $GFP^+/CD31^+$ and $\beta\text{-}Gal^+/CD31^+$ lesions (2.7- and 2.2-fold, respectively, $P<0.05$) in Epo-treated mice compared with the saline-treated mice (Figure 4A and 4B). The ratio of Epo-induced GFP^+ area in total $CD31^+$ regenerated endothelium was 31±0.3% (n=5) (Figure 4A), suggesting that Epo-mediated reendothelialization is composed of differentiation of BM-derived EPCs as well as facilitated proliferation of resident ECs. In addition, the numbers of BM-derived macrophages ($GFP^+/MOMA2^+$) and vascular smooth muscle cells ($GFP^+/\alpha SMA^+$) in the neointima of the Epo-treated mice were much lower than those of the control group (Figure 4A). $GFP^+/CD3^+$ or $GFP^+/B220^+$ cells were barely detectable in the neointima of both groups (data not shown).

Expression of EpoR in Epo-Treated Injured Artery

We investigated whether Epo-mobilized EPCs actually express the specific receptor for Epo (EpoR). EpoR-positive cells (brown staining, arrowheads in Figure 5A) were apparently localized on the regenerated endothelium in the Epo-treated arteries, whereas the expression of EpoR in the saline-treated injured or uninjured arteries was barely detectable.

The immunofluorescence study using anti-EpoR, anti-CD31, anti-CD45, and anti–αSM-actin (αSMA) antibodies revealed that $CD31^+$ endothelial cells in Epo-treated arteries coexpressed EpoR on the endothelial layer, whereas neither

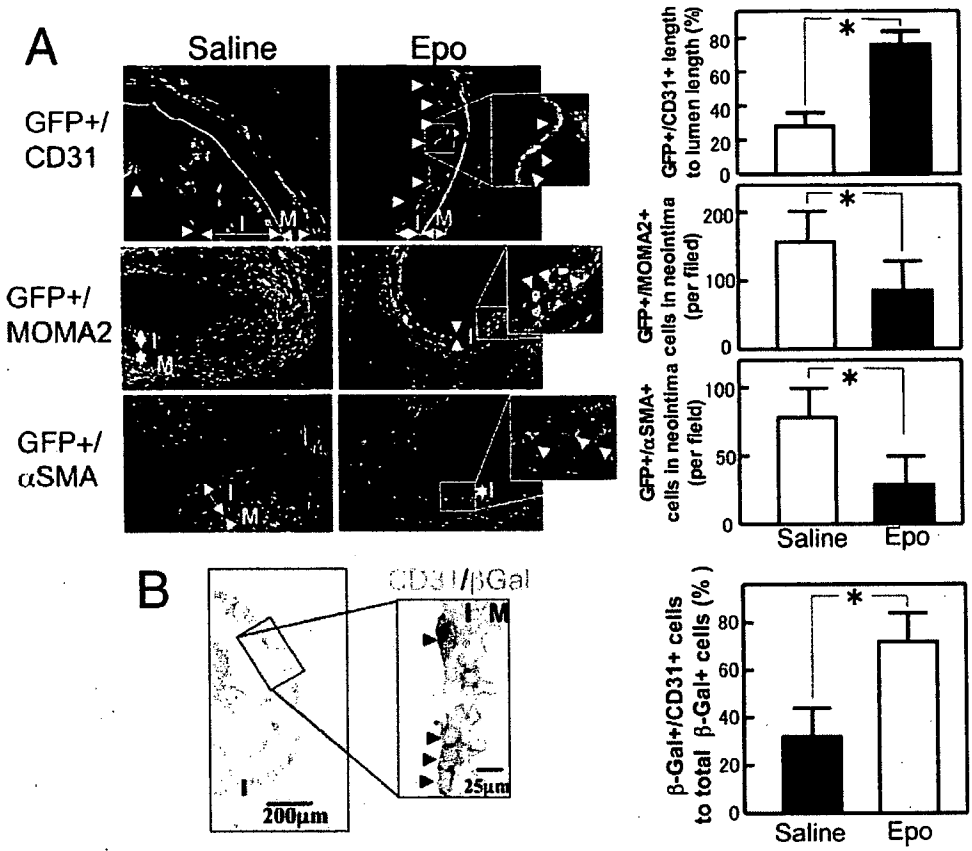

Figure 4. Incorporation of BM-derived cells into regenerated endothelium. A, BM cells from donor GFP–overexpressing mice were transfused to the irradiated recipient mice and subject to vascular injury. The day-14 samples were immunostained with antibodies against CD31, MOMA2, αSMA, and GFP. The localizations of double-fluorescent cells, including $GFP^+/CD31^+$, $GFP^+/MOMA2$, and $GFP^+/\alpha SMA$ cells, are shown as yellow dots in the merged image (arrowheads, bar=20 μm). Semiquantitative analysis of the double-fluorescent cell area per section is shown relative to the total lumen length or the number in the neointima (n=5 each, $^*P<0.02$). B, BM cells from donor β-Gal–overexpressing mice were transfused to the irradiated recipient mice and subjected to vascular injury. β-Gal–expressing cells (blue) and CD31$^+$ cells (brown) were observed in the day-14 samples. $\beta\text{-Gal}^+/CD31^+$ double-stained cells are indicated by arrowheads, and the relative ratio to total $\beta\text{-Gal}^+$ cells is shown (n=5 in each group, $^*P<0.05$).

$CD45^+$ cells nor αSMA^+ cells expressed EpoR (Figure 5B). We also confirmed the expression of EpoR in the BM-derived EC-like cells mobilized by Epo using the mice repopulated with GFP^+ BM cells (Figure 5C). Abundant $GFP^+/EpoR^+$ cells were detected on the luminal surface in the Epo-treated injured artery, and the distribution was 2.5-fold greater than that in the saline-treated mice ($P<0.05$, Figure 5D).

Epo Activates Akt-eNOS Pathways and NO Production in EPCs

To investigate whether PB and BM EPCs express EpoR, $Sca1^+/Flk\text{-}1^+$ EPCs were isolated from PB and BM by FACS and subjected to RT-PCR analysis. The DNA fragment corresponding to EpoR was amplified in the predicted size (Figure 6A). We further studied whether $Sca1^+/Flk\text{-}1^+$ EPCs have the ability to activate the EpoR/Akt/eNOS pathway in response to Epo treatment. Because the PB volume obtained from the mice is too little to get the sufficient number of endothelial-lineage cells attaching on the plate, and also the attaching mice-derived cells are less spreading and less proliferative compared with the human cells, we used the human PB EPCs. The $CD133^+$ EPCs were isolated from human PB by magnetic-associated cell sorting and primarily cultured. To study the stimulatory effect of Epo on the downstream pathway, after 12-hour serum starvation (0.5% serum), $CD133^+$ EPCs were treated with 1.2 IU/mL Epo for 30 minutes. Double staining using anti-EpoR with anti–phosphorylated Akt or anti–phosphorylated eNOS antibodies showed that Epo markedly induced Akt-eNOS phosphorylation in EpoR-positive EPCs (Figure 6B).

We further measured the intracellular NO level with DAF-FM DA (10 μmol/L). NO was visualized as a green dot under laser microscopy (Figure 6C). Epo stimulation upregulated NO level to 1.7-fold higher than the untreated control level ($P<0.05$), whereas addition of L-NAME completely abolished this increase.

Discussion

The balloon-mediated injury of endothelial integrity stimulates a regeneration of the EC monolayer, but this regenerative process is slow and cannot prevent the early proliferative events leading to the onset of a neointimal lesion. A novel approach that promotes early reendothelialization is required to potentiate this natural regenerative process. In this study, we examined whether Epo treatment is a feasible strategy to cause reendothelialization of wire-injured vessels. Our results

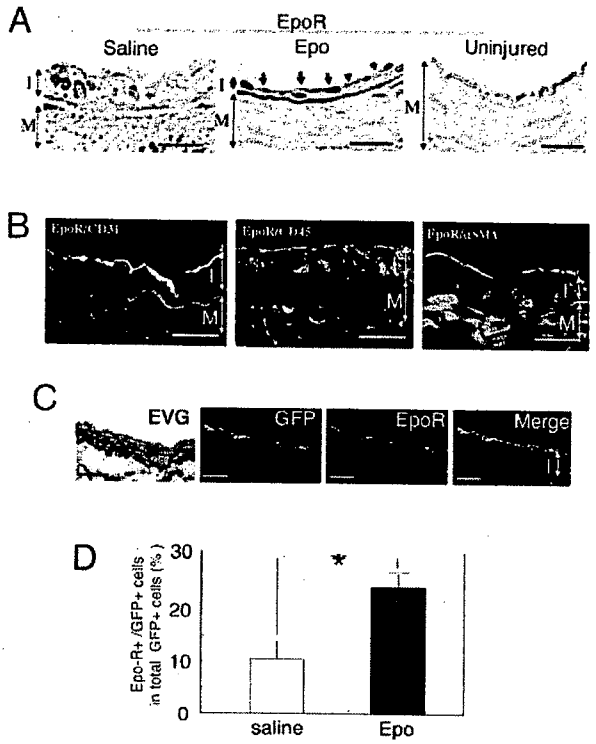

Figure 5. Localization and characterization of EpoR-expressing cells in neointima. A, Immunohistochemistry for EpoR showing the abundant localization of EpoR-expressing cells (brown, arrowheads) in the Epo-treated artery (day-14 sample) compared with saline-treated control and uninjured artery (bar=50 μm). B, Double-immunofluorescent images for EpoR (red) and CD31 (green, left), CD45 (green, middle), or αSMA (green, right) (bar=20 μm) showing coexpression of EpoR in $CD31^+$ cells. C, Localization of BM-derived EpoR-expressing cells in Epo-treated mice repopulated with GFP-overexpressing BM cells. Elastica van Gieson–stained sections (left) and immunofluorescent images for GFP (green) and EpoR (red) showing the localization of BM-derived $EpoR^+$ cells (yellow in merge image) along neointimal surface (bar=50 μm). D, Relative percentage of BM-derived EpoR-expressing cells in total BM-derived GFP^+ cells in the neointima (n=5 each, $^*P<0.05$). I indicates intima; M, media.

demonstrated that the 3-day treatment of Epo increases the circulating $Sca\text{-}1^+/Flk\text{-}1^+$ EPCs expressing an EpoR and that the mobilized EPCs contribute to the reendothelialization, leading to the inhibition of neointimal hyperplasia in an NO-dependent manner. Furthermore, we found that EpoR expression is upregulated in the Epo-induced neoendothelium and that the Epo/EpoR system causes the activation of the Akt-eNOS pathway on the EPCs and inhibits the apoptosis of medial SMCs.

EPCs can be harvested from PB, and intravenous transplantation of EPCs into EC-denuded vessels potentiates the recovery of endothelial integrity that causes the inhibition of neointimal hyperplasia,[4,8] although cell transplantation protocols, such as the ex vivo expansion of EPCs, are technically challenging. G-CSF–induced EPCs were shown to enhance the repair of injured arteries and prevent intimal hyperplasia.[18] However, it appears that the safety and feasibility of G-CSF treatment focusing on the induction of vascular occlusion in atherosclerotic lesions has not yet been established. In 12 intractable angina patients, the administration of G-CSF was associated with 2 cases of acute myocardial infarction and 1 case of cardiac death.[27] There are articles reporting the induction of acute myocardial infarction and cerebral infarction in G-CSF–treated BM transplantation patients.[28,29] Differentiation of G-CSF–mobilized progenitor cells into VSMC within the stented segment, induction of angiogenesis within the atherosclerotic lesion, and aggregation of mobilized inflammatory cells within the plaque may be plausible explanations.

This study showed that short-term (3-day) treatment with Epo after EC-denuded injury leads to accelerated reendothelialization and marked inhibition of neointimal formation. Figure 2A demonstrates that the ratio of reendothelialization by Epo and saline treatment is 73% and 41% on the total lumen area, respectively, whereas the coverage by $CD31^+$ marrow-derived cells on the reendothelialized lumen area is 75% and 32%, respectively (Figure 4B), indicating that 55% of Epo-mediated reendothelialized area is derived from marrow cells, and, in the saline-treated control, 13% of reendothelialized area is marrow-derived cells. Considering that Epo-mediated EPC mobilization (Figure 3) and reendothelialization (Figure 2) are NO dependent, it is suggested that EPC release via Epo and the endothelial differentiation in the repair process is partly involved in the observed reduction of neointima. Although the mobilization of EPC might be considered unfavorable for tumor growth, multiple clinical trials have recommended the use of Epo in chemotherapy-associated anemia or for longer survival among patients with multiple myeloma.[30] Thus, the safety and feasibility of Epo treatment has been established. Although it was a concern that erythropoiesis may increase the risk of thrombosis because of an elevation in blood viscosity or cause hypertension resulting from the induction of the vasoconstricting hormone endothelin-1,[31] thrombosis formation at the injured lesion in the Epo-treated group was similar to the saline-injected group, and blood pressure did not increase after short-term Epo-treatment (unpublished observation, 2005). Moreover, Epo was reported to attenuate cytokine production and inflammation in tissue ischemia by targeting cell apoptosis[32] or to induce cellular protection by activating Epo-EpoR signals involving Akt pathways,[33] consistent with the present result (Figure 6). These antiinflammatory and antiapoptotic cytoprotection actions associated with endothelial EpoR-mediated Akt/NO signaling may also contribute to the preventive effect of Epo on the neointimal hyperplasia.

EPC-like cells were reportedly derived from more differentiated $CD34^+$ or immature $CD133^+$ hematopoietic stem cells, as well as from PB MNCs or $CD14^+$ monocytes.[2,8,16] These EPC-like cells lose CD45 hematopoietic markers and express endothelial markers. Our present study clearly showed that $CD45^{dim}/Flk\text{-}1^+$ or $Sca1^+/Flk\text{-}1^+$ EPCs were mobilized by Epo, had a functional EC-like property in vitro, and contributed to endothelial regeneration after wire-mediated injury, suggesting this cell type is an EPC-like cell responsible for Epo-induced vascular repair. Thus, Epo treatment may be a novel strategy to inhibit the neointimal hyperplasia by directly acting on the injured vessels as well as mobilizing EPCs to the neoendothelium.

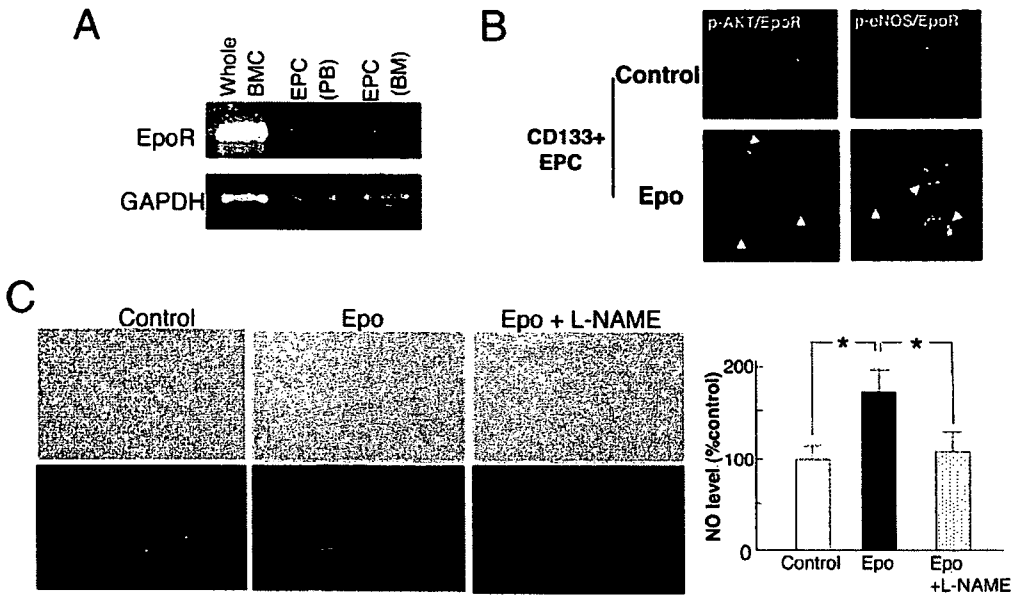

Figure 6. Epo-mediated activation of Akt/eNOS and NO production in PB-derived endothelial progenitor cells. A, The $Sca1^+/Flk\text{-}1^+$ EPCs were isolated from the PB and BM by FACS. Total RNAs were prepared from them and the whole BM cells and subsequently subjected to RT-PCR analysis using the primers for EpoR and GAPDH. The DNA fragments corresponding to EpoR and GAPDH were amplified in the predicted sizes. B, $CD133^+$ progenitor cells were purified to >90% purity from human PB MNCs by positive selection using anti-$CD133^+$ microbeads and a magnetic cell sorting device and then were primary cultured. After 12 hours of serum starvation (0.5% serum), they were stimulated by 1.2 IU/mL Epo for 30 minutes and immunostained for EpoR (green) with phosphorylated Akt kinase (red) or phosphorylated eNOS (red) (bar=25 μm). Double-fluorescence–positive cells appear yellow (arrowheads). C, Measurement of the intracellular NO level. The $CD133^+$ cells were loaded with DAF-FM DA (10 μmol/L), and NO was visualized as a green dot under laser microscopy. The averaged intensity in the Epo and the Epo plus L-NAME cells relative to the control group was evaluated. *P<0.005 (n=8, each).

Acknowledgments

This work was supported by a Grant from the Ministry of Education, Culture, Science and Technology of Japan.

References

1. Libby P, Schwartz D, Brogi E, Tanaka H, Clinton SK. A cascade model for restenosis. A special case of atherosclerosis progression. *Circulation.* 1992;86(suppl III):III-47–III-52.
2. Asahara T, Murohara T, Sullivan A, Silver M, van der Zee R, Li T, Witzenbichler B, Schatteman G, Isner JM. Isolation of putative progenitor endothelial cells for angiogenesis. *Science.* 1997;275:964–967.
3. Asahara T, Masuda H, Takahashi T, Kalka C, Pastore C, Silver M, Kearne M, Magner M, Isner JM. Bone marrow origin of endothelial progenitor cells responsible for postnatal vasculogenesis in physiological and pathological neovascularization. *Circ Res.* 1999;85:221–228.
4. Griese DP, Ehsan A, Melo LG, Kong D, Zhang L, Mann MJ, Pratt RE, Mulligan RC, Dzau VJ. Isolation and transplantation of autologous circulating endothelial cells into denuded vessels and prosthetic grafts: implications for cell-based vascular therapy. *Circulation.* 2003;108:2710–2715.
5. Fujiyama S, Amano K, Uehira K, Yoshida M, Nishiwaki Y, Nozawa Y, Jin D, Takai S, Miyazaki M, Egashira K, Imada T, Iwasaka T, Matsubara H. Bone marrow monocyte lineage cells adhere on injured endothelium in a monocyte chemoattractant protein-1-dependent manner and accelerate reendothelialization as endothelial progenitor cells. *Circ Res.* 2003;93:980–989.
6. Werner N, Junk S, Laufs U, Link A, Walenta K, Bohm M, Nickenig G. Intravenous transfusion of endothelial progenitor cells reduces neointima formation after vascular injury. *Circ Res.* 2003;93:e17–e24.
7. Kong D, Melo LG, Mangi AA, Zhang L, Lopez-Ilasaca M, Perrella MA, Liew CC, Pratt RE, Dzau VJ. Enhanced inhibition of neointimal hyperplasia by genetically engineered endothelial progenitor cells. *Circulation.* 2004a;109:1769–1775.
8. Gulati R, Jevremovic D, Peterson TE, Witt TA, Kleppe LS, Mueske CS, Lerman A, Vile RG, Simari RD. Autologous culture-modified mononuclear cells confer vascular protection after arterial injury. *Circulation.* 2003;108:1520–1526.
9. Anagnostou A, Liu Z, Steiner M, Chin K, Lee ES, Kessimian N, Noguchi CT. Erythropoietin receptor mRNA expression in human endothelial cells. *Proc Natl Acad Sci U S A.* 1994;91:3974–3978.
10. Anagnostou A, Lee ES, Kessimian N, Levinson R, Steiner M. Erythropoietin has a mitogenic and positive chemotactic effect on endothelial cells. *Proc Natl Acad Sci U S A.* 1990;87:5978–5982.
11. Carlini RG, Alonzo EJ, Dominguez J, Blanca I, Weisinger JR, Rothstein M, Bellorin-Font E. Effect of recombinant human erythropoietin on endothelial cell apoptosis. *Kidney Int.* 1999;55:546–553.
12. Beleslin-Cokic BB, Cokic VP, Yu X, Weksler BB, Schechter AN, Noguchi CT. Erythropoietin and hypoxia stimulate erythropoietin receptor and nitric oxide production by endothelial cells. *Blood.* 2004;103:921–926.
13. Heeschen C, Aicher A, Lehmann R, Fichtlscherer S, Vasa M, Urbich C, Mildner-Rihm C, Martin H, Zeiher AM, Dimmeler S. Erythropoietin is a potent physiologic stimulus for endothelial progenitor cell mobilization. *Blood.* 2003;102:1340–1346.
14. Ribatti D, Presta M, Vacca A, Ria R, Giuliani R, Dell'Era P, Nico B, Roncali L, Dammacco F. Human erythropoietin induces a pro-angiogenic phenotype in cultured endothelial cells and stimulates neovascularization in vivo. *Blood.* 1999;93:2627–2636.
15. Galeano M, Altavilla D, Cucinotta D, Russo GT, Calo M, Bitto A, Marini H, Marini R, Adamo EB, Seminara P, Minutoli L, Torre V, Squadrito F. Recombinant human erythropoietin stimulates angiogenesis and wound healing in the genetically diabetic mouse. *Diabetes.* 2004;53:2509–2517.
16. Kalka C, Masuda H, Takahashi T, Gordon R, Tepper O, Gravereaux E, Pieczek A, Iwaguro H, Hayashi SI, Isner JM, Asahara T. Vascular endothelial growth factor165 gene transfer augments circulating endothelial progenitor cells in human subjects. *Circ Res.* 2000;86:1198–1202.
17. Kocher AA, Schuster MD, Szabolcs MJ, Takuma S, Burkhoff D, Wang J, Homma S, Edwards NM, Itescu S. Neovascularization of ischemic myocardium by human bone-marrow-derived angioblasts prevents cardiomyocyte apoptosis, reduces remodeling and improves cardiac function. *Nat Med.* 2001;7:430–436.
18. Kong D, Melo LG, Gnecchi M, Zhang L, Mostoslavsky G, Liew CC, Pratt RE, Dzau VJ. Cytokine-induced mobilization of circulating endothelial progenitor cells enhances repair of injured arteries. *Circulation.* 2004b;110:2039–2046.

19. Sata M, Saiura A, Kunisato A, Tojo A, Okada S, Tokuhisa T, Hirai H, Makuuchi M, Hirata Y, Nagai R. Hematopoietic stem cells differentiate into vascular cells that participate in the pathogenesis of atherosclerosis. *Nat Med.* 2002;8:403–409.
20. Okabe M, Ikawa M, Kominami K, Nakanishi T, Nishimune Y. 'Green mice' as a source of ubiquitous green cells. *FEBS Lett.* 1997;407:313–319.
21. Zambrowicz BP, Imamoto A, Fiering S, Herzenberg LA, Kerr WG, Soriano P. Disruption of overlapping transcripts in the ROSA beta geo 26 gene trap strain leads to widespread expression of beta-galactosidase in mouse embryos and hematopoietic cells. *Proc Natl Acad Sci U S A.* 1997;94:3789–3794.
22. Hori T, Matsubara T, Ishibashi T, Yamazoe M, Ida T, Higuchi K, Takemoto M, Ochiai S, Tamura Y, Aizawa Y, Nishio M. Decrease of nitric oxide end-products during coronary circulation reflects elevated basal coronary artery tone in patients with vasospastic angina. *Jpn Heart J.* 2000;41:583–595.
23. Urbich C, Heeschen C, Aicher A, Sasaki K, Bruhl T, Farhadi MR, Vajkoczy P, Hofmann WK, Peters C, Pennacchio LA, Abolmaali ND, Chavakis E, Reinheckel T, Zeiher AM, Dimmeler S. Relevance of monocytic features for neovascularization capacity of circulating endothelial progenitor cells. *Circulation.* 2003;108:2511–2516.
24. Moroi M, Zhang L, Yasuda T, Virmani R, Gold HK, Fishman MC, Huang PL. Interaction of genetic deficiency of endothelial nitric oxide, gender, and pregnancy in vascular response to injury in mice. *J Clin Invest.* 1998;101:1225–1232.
25. Sata M, Maejima Y, Adachi F, Fukino K, Saiura A, Sugiura S, Aoyagi T, Imai Y, Kurihara H, Kimura K, Omata M, Makuuchi M, Hirata Y, Nagai R. A mouse model of vascular injury that induces rapid onset of medial cell apoptosis followed by reproducible neointimal hyperplasia. *J Mol Cell Cardiol.* 2000;32:2097–2104.
26. Beohar N, Flaherty JD, Davidson CJ, Maynard RC, Robbins JD, Shah AP, Choi JW, MacDonald LA, Jorgensen JP, Pinto JV, Chandra S, Klaus HM, Wang NC, Harris KR, Decker R, Bonow RO. Antirestenotic effects of a locally delivered caspase inhibitor in a balloon injury model. *Circulation.* 2004;109:108–113.
27. Hill JM, Syed MA, Arai AE, Powell TM, Paul JD, Zalos G, Read EJ, Khuu HM, Leitman SF, Horne M, Csako G, Dunbar CE, Waclawiw MA, Cannon RO 3rd. Outcomes and risks of granulocyte colony-stimulating factor in patients with coronary artery disease. *J Am Coll Cardiol.* 2005; 46:1643–1648.
28. Fukumoto Y, Miyamoto T, Okamura T, Inaba S, Harada M, Niho Y. Angina pectoris occurring during granulocyte colony-stimulating factor-combined preparatory regimen for autologous peripheral blood stem cell transplantation in a patient with acute myelogenous leukaemia. *Br J Haematol.* 1997;97:666–668.
29. Kawachi Y, Watanabe A, Kurooka N, Setsu K. Acute arterial thrombosis due to platelet aggregation in a patient receiving granulocyte colony-stimulating factor. *Br J Haematol.* 1996;94:413–416.
30. Rizzo JD, Lichtin AE, Woolf SH, Seidenfeld J, Bennett CL, Regan DH, Browman GP, Gordon MS; American Society of Clinical Oncology; American Society of Hematology. Use of epoetin in patients with cancer: evidence-based clinical practice guidelines of the American Society of Clinical Oncology and the American Society of Hematology. *Blood.* 2002;100:2303–2320.
31. Vogel V, Kramer HJ, Backer A, Meyer-Lehnert H, Jelkmann W, Fandrey J. Effects of erythropoietin on endothelin-1 synthesis and the cellular calcium messenger system in vascular endothelial cells. *Am J Hypertens.* 1997;10:289–296.
32. Genc S, Koroglu TF, Genc K. Erythropoietin as a novel neuroprotectant. *Res Neurol Neurosci.* 2004;22:105–119.
33. Chong ZZ, Kang JQ, Maiese K. Erythropoietin is a novel vascular protectant through activation of Akt1 and mitochondrial modulation of cysteine proteases. *Circulation.* 2002;106:2973–2979.

Granulocyte Colony-Stimulating Factor–Mobilized Circulating c-Kit+/Flk-1+ Progenitor Cells Regenerate Endothelium and Inhibit Neointimal Hyperplasia After Vascular Injury

Michitaka Takamiya, Mitsuhiko Okigaki, Denan Jin, Shinji Takai, Yoshihisa Nozawa, Yasushi Adachi, Norifumi Urao, Kento Tateishi, Tetsuya Nomura, Kan Zen, Eishi Ashihara, Mizuo Miyazaki, Tetsuya Tatsumi, Tomosaburo Takahashi, Hiroaki Matsubara

Background—Granulocyte colony-stimulating factor (G-CSF) treatment was shown to inhibit neointimal formation of balloon-injured vessels, whereas neither the identification of progenitor cells involved in G-CSF–mediated endothelial regeneration with a bone marrow (BM) transplant experiment nor the functional properties of regenerated endothelium have been studied.

Methods and Results—Recombinant human G-CSF (100 μg/kg per day) was injected daily for 14 days starting 3 days before balloon injury in the rat carotid artery. Neointimal formation of denuded vessels on day 14 was markedly attenuated by G-CSF (39% versus the control; $P<0.05$). Endothelial cell–specific immunostaining revealed an enhancement of re-endothelialization (1.8-fold increase versus the control; $P<0.05$) and inhibition of extravasation of Evans Blue dye (47%; $P=0.02$). The regenerated endothelium exhibited acetylcholine-mediated vasodilatation in NO-dependent manner. G-CSF increased the circulating c-Kit+/Flk-1+ cells (9.1-fold; $P<0.02$), which showed endothelial properties in vitro (acetylated low-density lipoprotein uptake and lectin binding) and incorporated into the regenerated endothelium in vivo. A BM replacement experiment with green fluorescent protein (GFP)–overexpressing cells showed that BM-derived GFP+/CD31+ endothelial cells occupied 39% of the total luminal length in the G-CSF–mediated neo-endothelium (2% in the control).

Conclusion—The G-CSF–induced mobilization of BM-derived c-Kit+/Flk-1+ cells contributes to endothelial regeneration, and this cytokine therapy may be a feasible strategy for the promotion of re-endothelialization after angioplasty. (***Arterioscler Thromb Vasc Biol.* 2006;26:751-757.**)

Key Words: restenosis ■ endothelium ■ carotid artery ■ cytokines ■ vascular biology

Endothelial cells (ECs) cover the luminal surface of blood vessels and maintain multiple vascular functions. The disruption of endothelial coverage causes a decrease in the production of vasculoprotective mediators such as NO, leading to elevated vascular tonus, enhanced inflammation, and medial smooth muscle cell proliferation. The resultant neointimal hyperplasia causes restenosis after angioplasty.[1]

Bone marrow (BM)–derived endothelial progenitor cells (EPCs) was isolated from the mononuclear cell (MNC) population in the peripheral blood (PB).[2,3] Transplantation of autologous circulating EPCs (CEPCs) to balloon-denuded arteries was reported to induce rapid re-endothelialization of the injured artery.[4,5] Moreover, transfusion of spleen-derived EPCs or EPCs overexpressing endothelial NO synthase reduced neointimal formation after vascular injury.[6,7] Delivery of cultured PB-MNCs to balloon-injured arteries accelerated re-endothelialization associated with endothelium-dependent vasoreactivity and reduced neointimal formation.[7]

Cytokines efficiently mobilize hematopoietic precursor cells from BM.[8] Takahashi et al showed that exogenous granulocyte/macrophage colony-stimulating factor (CSF) mobilize CEPCs from BM and thereby contributes to neovascularization of ischemic tissues.[9] Recently, granulocyte-CSF (G-CSF) was shown to recruit BM-derived EPCs[10] and enhance the BM cell mobilization to brain, leading to angiogenesis and eventually a reduction in the volume of cerebral infarction.[11] G-CSF was also reported to increase angiogenesis in the BM of G-CSF–treated patients.[12] Treatment with

Original received June 6, 2005; final version accepted December 15, 2005.

From the Department of Cardiovascular Medicine (M.T., M.O., N.U., K.T., T.N., K.Z., E.A., T. Tatsumi, T. Takahashi, H.M.), Kyoto Prefectural University School of Medicine, Japan; Department of Pharmacology (D.J., S.T., M.M.), Osaka Medical College, Takatsuki, Japan; Pharmacobioregulation Research Laboratory (Y.N.), Taiho Pharmaceutical Co. Ltd. Saitama, Japan; and Department of Pathology II (Y.A.), Kansai Medical University, Moriguchi, Japan.

Correspondence to Mitsuhiko Okigaki MD, Department of Cardiovascular Medicine, Kyoto Prefectural University of Medicine, Kamigyo-ku, Kyoto, 602-8566, Japan. E-mail okigakim@koto.kpu-m.ac.jp

Arterioscler Thromb Vasc Biol. is available at http://www.atvbaha.org DOI: 10.1161/01.ATV.0000205607.98538.9a

G-CSF plus macrophage CSF accelerates neovascularization in limb ischemia.[13] G-CSF enhances endothelialization of small-caliber prosthetic implanted grafts,[14,15] and intracoronary infusion of G-CSF–mobilized PB-MNCs improved cardiac regional flow in patients with myocardial infarction.[16] Kong et al reported that mobilization of CEPCs by exogenous G-CSF facilitates re-endothelialization and inhibits neointimal development,[17] whereas the cell types of BM-derived cells contributing to G-CSF–mediated endothelial regeneration in the vascular repair model has not been defined in a BM transplant experiment, and neither the involvement of G-CSF–mediated outgrowth of resident ECs bordering the injured area nor the functional properties of the regenerated endothelium were studied in G-CSF–treated animals. To further elucidate these undetermined issues, the present study was designed, and it provided the additional novel findings that: (1) BM-derived c-Kit+/Flk-1+ progenitor cells mobilized by G-CSF directly contribute to the endothelial regeneration after EC-denuded injury and can differentiate to EC-like cells in vitro, (2) the contribution of the G-CSF–mediated outgrowth of resident ECs is negligible, and (3) the repaired artery showed NO-mediated arterial relaxation and inhibition of neointimal hyperplasia. These findings suggested that G-CSF therapy can be a feasible therapy to inhibit neointimal hyperplasia after angioplasty.

Materials and Methods

Balloon Injury Model

A 2Fr Fogarty arterial embolectomy catheter (Edwards Lifesciences) was inserted into the right common carotid artery of Lewis rats (LEW/SsN Slc; 10 to 12 weeks of age) and inflated 3 times with 300 μL of air. Human G-CSF (Lenograstim; 10, 30, or 100 μg/kg per day) or vehicle (saline) was subcutaneously injected daily for 14 days from 3 days before injury. The lesion was harvested on day 14. Green fluorescent protein (GFP) transgenic mice were generously donated by Dr Okabe (Osaka University, Japan).[18] All experimental procedures complied with the institutional guidelines for animal experiments.

Morphometric Analysis

The injured lesion was fixed with 4% paraformaldehyde, paraffin sectioned, and stained with hematoxylin and eosin or Elastica van Gieson. Three sections from each carotid artery at 300-μm intervals were analyzed with NIH image software. The absolute intimal area or relative ratio of intimal-to-medial area (I/M ratio) was evaluated. Evans blue dye (5%; Sigma) was transfused to rats 10 minutes before euthanasia to identify the remaining denuded area. Furthermore, to analyze the EC-recovered area, samples were incubated with horseradish peroxidase (HRP)–conjugated anti-FactorVIII antibody, followed by visualization with 3, 3′-diaminobenzidine (DAB). Slides were then counterstained with hematoxylin.

Functional Assay of Regenerated Endothelium

NO-mediated vasorelaxation of regenerated endothelium was evaluated as we described previously.[5]

Transfusion of G-CSF–Induced PB-MNCs

PB-MNCs were isolated by Percoll gradient centrifugation (Lymphoprep; NYCOMED) from 5-day G-CSF–treated donor rats and labeled with DiI[19] and transfused to the recipient Lewis rat after arterial injury (1×10^7 cells). After a 5-day G-CSF treatment in GFP-overexpressing mice, PB-MNCs were prepared and incubated with phycoerythrin (PE)–Cy5-conjugated anti-mouse CD45 or anti-mouse c-Kit antibodies (BD Pharmingen), as well as PE-conjugated anti-mouse Flk-1 (Becton Dickinson). GFP+/c-Kit+/Flk-1+ and GFP+/c-Kit+/Flk-1− cells were sorted and transfused to the recipient nude rats (F344/N rnu/rnu) after arterial injury. On day 14, the lesion was frozen sectioned and incubated with anti-CD31 antibody (Santa Cruz Biotechnology), followed by rhodamine-conjugated secondary antibody (DAKO).

Primary Culture of G-CSF–Induced PB-MNCs

PB-MNCs were prepared from 5-day G-CSF–treated rats and cultured on fibronectin-coated chamber slides (Becton Dickinson) for 7 days with 10% FBS-DMEM (GIBCO). Adherent cells were incubated with 2.4 μL/mL of DiI-labeled acetylated LDL (Molecular Probes) for 120 minutes, fixed with 2% paraformaldehyde, and stained with 10 ng/mL of fluorescein isothiocyanate (FITC)–conjugated Ulex europaeus agglutinin-1 (UEA-1) lectin (Sigma). The double fluorescent cells were counted in 4 randomly selected high-power fields.

Fluorescence-Activated Cell Sorter Analysis of G-CSF–Induced Mice PB-MNCs

PB-MNCs were prepared from 5-day G-CSF–treated C57BL/6 mice, incubated with PE-conjugated antibody against CD3, CD8, B220, CD11b, Ter119 or Gr-1, and FITC-conjugated anti-CD34 antibody as well as biotin-conjugated mouse antibody against Flk-1 or c-Kit, followed by activated protein C–conjugated secondary antibody (all from Pharmingen). Samples were analyzed with fluorescent-activated cell sorter (FACS) caliber using Cell Quest (Becton Dickinson).

BM Transplantation

1×10^7 BM cells from GFP-overexpressing mice were transplanted to nude rats (F344/N rnu/rnu) after 6 Gray irradiation. At week 4, arterial injury was conducted, and G-CSF (100 μg/kg per day) was injected daily for 14 days from 3 days before arterial injury. The lesions were frozen sectioned and stained with anti-CD31 antibody with rhodamine-conjugated secondary antibody (DAKO).

Immunohistochemistry

The injured lesions were paraffin sectioned at 14 days after balloon injury and immunostained with anti-rat CD45 (BD Pharmingen) and rat cross-reactive anti–interleukin-1β (IL-1β) antibodies (sc-7884; Santa Cruz Biotechnology) and HRP-conjugated secondary antibody, followed by visualization with DAB and counterstained with hematoxylin.

Statistical Analysis

Statistical analyses were performed with 1-way ANOVA followed by pairwise contrasts using Dunnett test. Data (means±SE) were considered statistically significant when P was <0.05.

Results

G-CSF Inhibits Neointimal Hyperplasia After Arterial Injury

We determined whether G-CSF treatment inhibits neointimal hyperplasia after EC-denuded balloon injury of carotid artery. Neointimal lesions developed in the vehicle-treated vessels 2 weeks after injury, whereas G-CSF treatment markedly reduced the neointimal formation in a dose-dependent manner (10 to 100 μg/kg per day; Figure 1). Morphometric analysis revealed a remarkable decrease in the neointimal area of high-dose G-CSF (100 μg/kg per day)–treated rats compared with the vehicle-treated group (39±3% decrease; n=10; $P<0.05$). The I/M ratio in G-CSF–treated rats was less than that in the vehicle-treated group (46.0±7.6% versus 84.3±7.3%; n=10; $P<0.05$; Figure 1B). Thus, it is unlikely that G-CSF directly affects the outgrowth of resident smooth

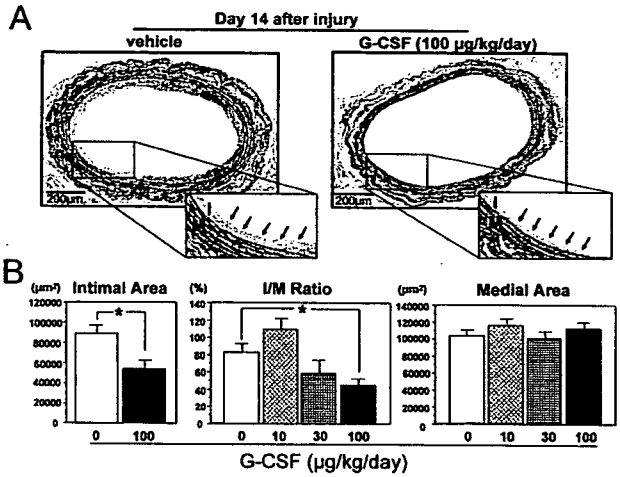

Figure 1. G-CSF inhibits neointimal hyperplasia after EC-denuded balloon injury. Endothelial denudation of rat carotid artery was induced by balloon catheter (day 0). The rats were injected with G-CSF: 0 μg/kg per day (vehicle only), 10, 30, or 100 μg/kg per day (n=10, each group). A, G-CSF (100 μg/kg per day) was subcutaneously injected daily for 14 days from 3 days before arterial injury. On day 14, the injured lesion was stained with Elastica van Gieson and subjected to morphometrical analysis. Arrows indicate apparent neointimal hyperplasia in the vehicle-injected group and marked inhibition of neointimal lesions in the G-CSF–treated group. B, Statistical analysis: intimal (I) or medial area (M) as well as the I/M ratio were evaluated 14 days after balloon injury with NIH image software. *$P<0.05$ vs vehicle-injected groups (n=10).

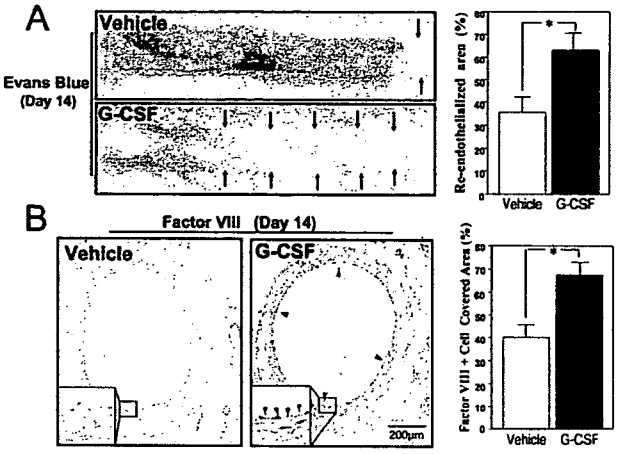

Figure 2. G-CSF facilitates re-endothelialization after EC-denuded injury. A, At 14 days after balloon injury, Evans blue dye was intravenously injected before euthanization. The re-endothelialized area, which appears white (arrows), was significantly larger in the G-CSF group than in the vehicle-treated group. *$P<0.05$ vs vehicle-injected group (n=6). B, On day 14, the injured lesion was immunostained with HRP-conjugated anti-FactorVIII antibody, followed by visualization with DAB. The FactorVIII+ cell-covered area (arrowheads) to the total length of luminal surface (%) in the G-CSF–treated group was significantly greater than in the vehicle-injected group. *$P<0.05$ vs vehicle-treated group (n=6).

muscle cells in the injured artery in vivo, although G-CSF was reported to stimulate the growth of the cultured vascular smooth muscle cells.[20]

We also studied whether G-CSF aggravated inflammatory cell infiltration and cytokine expression in the injured arteries by examining the infiltration of inflammatory cells (CD45+ cells) and the expression of inflammatory cytokine (IL-1β) in the injured arteries. Figure I (available online at http://atvb.ahajournals.org) shows that the infiltration of CD45+ cells and the expression of IL-1β are markedly inhibited in the day-14 neoendothelium of G-CSF–treated rats compared with those in the saline-treated controls, consistent with the previous observation that G-CSF pellet–induced angiogenic activity on the cornea occurred without any sign of inflammatory reactions.[21]

G-CSF treatment dose dependently (10, 30, and 100 μg/kg per day) elevated the number of white blood cells 14 days after treatment (14 500±2000, 19 660±430, 33 520±2171 cells; n=15 each), which were significantly higher compared with the vehicle-injected control (3640±153; n=15; $P<0.01$). Any dose of G-CSF (10, 30, or 100 μg/kg per day) did not affect the survival rate and body weight of the administrated rats and did not cause any macroanatomic change. Because 100 μg/kg per day of human G-CSF used here is considered to be similar to the human clinical dose based on the species difference between human and rodents,[22] and therefore this dose was used in the following experiment.

G-CSF Promotes Re-Endothelialization

To evaluate re-endothelialization, Evans Blue dye was administered premortem to stain-remaining nonendothelialized areas. Re-endothelialized areas appear white (Figure 2A) and were significantly larger in G-CSF–treated rats than in the vehicle-injected group (63.0±6.8% versus 35.7±6.6%; n=10; $P<0.01$). Immunostaining revealed that the ratio of FactorVIII+ endothelial layer relative to the total luminal surface was significantly greater in G-CSF–treated rats than in the control (67.4±7.9% versus 40.2±6.9%; n=10; $P<0.01$; Figure 2B), indicating that G-CSF promoted re-endothelialization, leading to the inhibition of neointimal hyperplasia.

Functional Analysis of Regenerated Endothelium

NO production in the regenerated endothelium was measured by acetylcholine (Ach)-mediated relaxation of carotid artery preconstricted by norepinephrine. Ach caused a relaxation response in the normal carotid artery (30.9±1.8%, n=6) versus papaverine-induced maximal relaxation in an NO-dependent manner (as shown by N^G-nitro-L-arginine methyl ester [L-NAME] inhibition), whereas in the EC-injured artery, this response was markedly abolished (2.8±0.9%, n=6). In contrast, in the G-CSF–treated injured artery, relaxation was restored to a level comparable to that of normal carotid artery (43.8±4.5%; n=6), whereas L-NAME pretreatment completely inhibited such an Ach-mediated response (Figure 3), suggesting that the regenerated endothelium exerts an NO-mediated vasorelaxation response.

Endothelial Regeneration by G-CSF–Mobilized CEPCs

Because G-CSF was reported to increase CEPCs,[10,17] we next examined whether the G-CSF–mobilized CEPCs actually contributed to endothelial regeneration after EC-denuded injury. PB-MNCs (1×10^7 cells) were prepared from 5-day

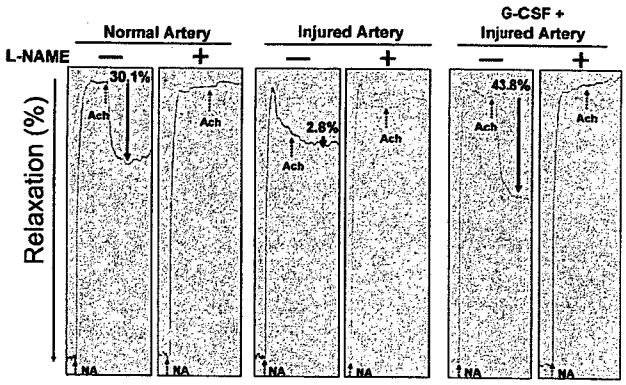

Figure 3. Ach-mediated relaxation of the carotid artery. Ach (10 μmol/L)-induced relaxation was examined using the carotid artery preconstricted with norepinephrine (30 nmol/L). The relaxation response was evaluated as a value relative to the papaverine-induced maximal relaxation (%) with or without L-NAME. Broken arrows show the time points to indicate drug administration. Solid arrows indicate Ach-induced vasorelaxation. Experiments were repeated 3 times with reproducible results. Representative data are shown.

G-CSF–treated or vehicle-injected donor rats, DiI-labeled, and transfused into the recipient rats after vascular injury. In the day-14 samples, DiI+ cells were incorporated into the neo-endothelium and double immunofluorescence with anti-CD31 antibody disclosed that DiI+ PB-MNCs derived from G-CSF–treated donor rats contributed to neoendothelium formation greater than the vehicle-injected rats (DiI+/CD31+ area 54.3±6.1% versus 6.3±1.2% to total luminal surface length; n=5; $P<0.01$; Figure 4A).

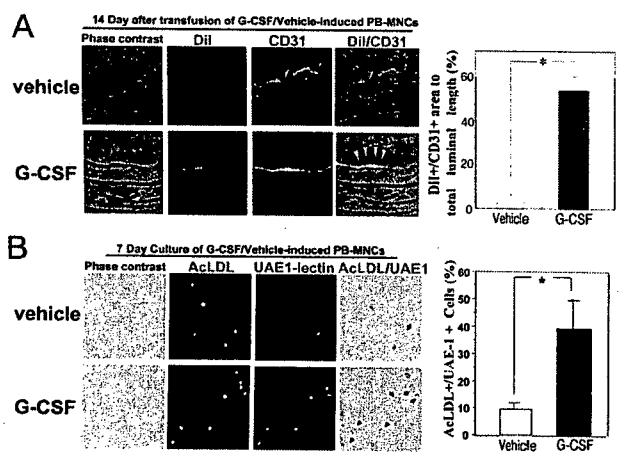

Figure 4. G-CSF increased the number of CEPCs. A, PB-MNCs were isolated from 5-day G-CSF–treated donor rats and labeled with DiI and transfused to the recipient rat after arterial injury (1×10^7 cells). On day 14, the injured lesion was removed, frozen-sectioned, and immunostained with FITC-conjugated anti-CD31 antibody. Localization of CD31+/DiI+ cells is indicated as yellow fluorescence in the merged image (arrowheads). Statistics: DiI+/CD31+ double fluorescent area in G-CSF–treated rat is greater than the vehicle-injected rat. *$P<0.05$ vs vehicle-treated group (n=6). B, PB-MNCs were cultured on fibronectin-coated plates for 7 days. EPC was identified with its binding ability to FITC–UAE-1-lectin and incorporation of DiI-AcLDL. Localization of UAE-1+/AcLDL+ cells is indicated by arrowheads in the merged image. Statistics: Percentage of double fluorescent cells relative to total adherent cells is presented (n=5; *$P<0.05$).

PB-MNCs from G-CSF–treated or vehicle-injected rats were primarily cultured for 7 days. EPC-like cells were identified by their binding ability to FITC–UEA1-lectin and uptake of DiI–AcLDL. The ratio of UAE-1+/AcLDL+ cells to total adherent cells from G-CSF–treated rats was 4-fold higher than that from vehicle-injected rats (39.2±9.8% versus 9.5±5.0% to total cultured cells; n=6; $P<0.05$; Figure 4B).

Endothelial Regeneration by G-CSF–Mobilized c-Kit+/Flk-1+ Cells

We studied the cell type responsible for endothelial regeneration induced by G-CSF. Because the anti-rat Flk-1 antibody for FACS sorting was not available, we analyzed the PB from "mice." Hematopoietic lineage negative (Lin-)/c-Kit+ cells were sorted from the mice PB and further analyzed for the expression of endothelial lineage markers Flk-1 and CD34. G-CSF treatment markedly elevated the ratio of Lin-/c-Kit+ cells to total PB-MNCs (8.1±0.5-fold; n=5; $P<0.01$), whereas the CD34+/Flk-1+ population included in the Lin-/c-Kit+ cells was increased 9.8±0.8-fold (n=5; $P<0.01$; Figure 5A).

To further elucidate the contribution of circulating c-Kit+/Flk-1+ cells to endothelial regeneration, 5×10^4 c-Kit+/Flk-1+/GFP+ or 1×10^6 c-Kit+/Flk-1-/GFP+ cells were isolated from enhanced GFP (EGFP) transgenic mice and injected into the nude rats after balloon injury. GFP mRNA transcription in the transgenic mice is driven by the chicken β-actin promoter and cytomegalovirus enhancer, indicating that the transcript expression in the hematopoietic and EC lineages is strong enough to trace them in the recipient mouse organ. In fact, GFP-positive ECs can be detected with a strong signal in the neo-endothelium. Figure 5B shows that GFP+ cells in the day-14 samples were detected on the regenerated endothelium of c-Kit+/Flk-1+ cell–transfused nude rats, and that these GFP+ cells were positive for the EC marker CD31 (Figure 5B, top, arrowheads), whereas the GFP+ cells were barely detectable in c-Kit+/Flk-1− cell–transfused nude rats (Figure 5B, bottom), suggesting that c-Kit+/Flk-1+ cells contain the cell population that can differentiate into CD31+ EC-like cells in the EC-denuded lesion.

Analysis by BM Replacement Model

To examine whether G-CSF–mobilized EPCs were originated from the BM, BM cells from EGFP transgenic mice were transplanted into the nude rats of which marrow cells had been ablated with whole body irradiation. Six weeks after transplantation, 86±2% of PB-MNCs were replaced (FACS; data not shown). The nude rats that received arterial injury and mobilization of BM-derived GFP+ cells to the neo-endothelium was examined on day 14. GFP+ cells were detected in the endothelial layer, and the immunostaining disclosed that CD31+/GFP+ EC-like cells were detected only in the G-CSF–treated group but not in the vehicle-injected group (39.2±5.8% versus 2.2±1.5% to total luminal surface length; n=5 each; $P<0.005$; Figure 6), indicating that 37.0% of the total luminal area (39.2% G-CSF group)−(2.2% saline group) was derived from G-CSF–mobilized BM cells (GFP+/CD31+ area). Considering that G-CSF–promoted neo-endothelium was 37.2% of the total luminal area (67.4%

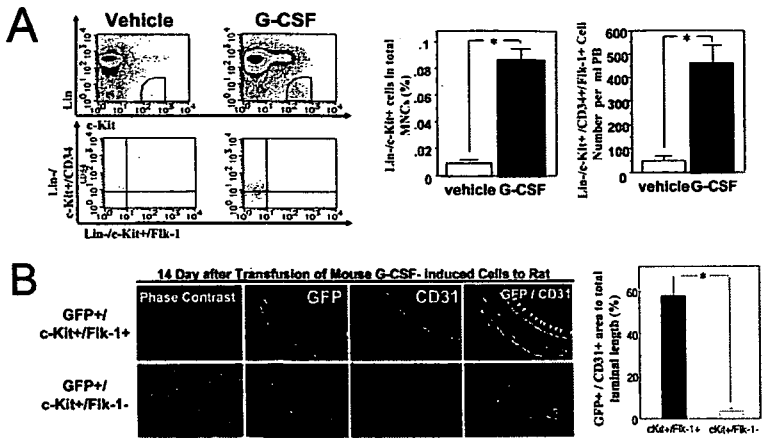

Figure 5. G-CSF–induced circulating c-Kit+/Flk-1+ cells differentiate to EC-like cells in the neo-endothelium. A, Five days after the injection of G-CSF, PB-MNCs were isolated, incubated with monoclonal antibodies (CD3-FITC, B220-FITC, CD11b-FITC, Gr1-FITC, NK1.1-FITC, Ter119-FITC, VEGFR-2-PE, and c-Kit-PE-Cy5) or with CD34-biotin, followed by activated protein C–avidine conjugated secondary antibody, and subjected to FACS analysis. The Lin-/c-Kit+ cell population was once gated (top left column) and subsequently analyzed for the expression of CD34 and Flk-1 (bottom left column). Statistical analysis: Percentage of Lin-/c-Kit+ cells to total MNCs or the absolute number of Lin-/c-Kit+/CD34+/Flk-1+ (right 2 panels) is significantly higher in G-CSF–treated group (n=5; *$P<0.01$ vs vehicle-injected group). B, Five days after the injection of G-CSF to GFP-overexpressing mice, PB-MNCs were collected, and 5×10^4 GFP+/c-Kit+/Flk-1+ or 1×10^6 GFP+/c-Kit+/Flk-1− cells were sorted and transfused to the nude rats after balloon injury. The lesion was removed on day 14, frozen sectioned, and subjected to immunostaining with rhodamine-conjugated antibody against CD31. CD31+/GFP+ cells appeared yellow in the merged image (arrowheads). *$P<0.01$ vs vehicle-treated group (n=5).

G-CSF group)−(40.2% saline group), these findings suggest that BM-derived cells are mainly involved in G-CSF–promoted neoendothelial formation, and the contribution of the G-CSF–mediated outgrowth of resident ECs is negligible.

Discussion

Because the natural regenerative process after EC-denuded injury is slow, it cannot prevent the onset of the neointimal lesions.[1] A novel approach that promotes re-endothelialization is required to accelerate this process. Several reports have shown that EPCs can be harvested from PB, and the intravenous injection of EPCs into EC-denuded vessels accelerates the recovery of endothelial integrity, resulting in the inhibition of neointimal hyperplasia and the restoration of vasodilatation activity.[4–7] The EPCs were shown to enhance the endothelialization of small-caliber prosthetic grafts.[14,15] G-CSF treatment increases the circulating CD34+ cells expressing endothelial markers,[10] and administration of G-CSF to patients with coronary artery disease increased the circulating MNCs with EPC properties.[23] Furthermore, G-CSF inhibited the neointimal formation in balloon-injured vessels,[17] whereas it remains undetermined what cell types of marrow-derived cells are directly involved in G-CSF–mediated endothelial regeneration. Furthermore, neither the functional properties of the regenerated endothelium were studied nor analysis using BM transplant experiments undertaken in G-CSF–treated animals. Our present study performed BM replacement experiments and clearly showed that G-CSF treatment increases the number of BM-derived c-Kit+/Flk-1+ EPCs that actually contribute to re-endothelialization of the balloon-injured arteries, leading to marked inhibition of neointimal formation. Furthermore, we found that the regenerated endothelium exerts Ach-mediated vasodilatory action in an NO-dependent manner. Interestingly, the injured arteries of G-CSF–treated rats have a better vasodilatory capacity compared with normal arteries. The data were analyzed in the 6 different animals with the reproducibility. Although we cannot sufficiently explain the molecular mechanism responsible for the better vasodilatory capacity, the neo-endothelium regenerated by G-CSF–mobilized BM cells or G-CSF–mediated direct action to the endothelial regeneration process might have the enhanced NO-mediated vasodilatory effect. Further studies will be required to clarify the underlying

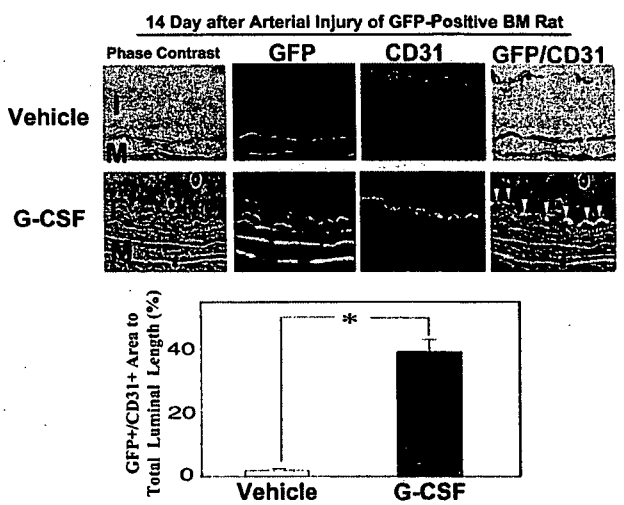

Figure 6. G-CSF–induced regenerated endothelium was originated from BM. Donor BM from EGFP-overexpressing mice was transfused to the BM-ablated nude rats. Recipient rats were balloon injured, and G-CSF or vehicle was injected daily for 14 days from 3 days before arterial injury. On day 14, the lesions were removed and immunostained with rhodamine-conjugated anti-CD31 antibody. CD31+/GFP+ cells appeared yellow in the merged image (arrowheads). Double fluorescent cells were detected on the neoendothelium in the G-CSF–treated nude rats (bottom panels), whereas they were barely detectable in the vehicle-treated nude rats (top panels). *$P<0.005$ vs vehicle-treated group (n=5).

mechanism. Together, this evidence leads us to consider a more aggressive clinical use of G-CSF to mobilize CEPCs and promote vascular repair.

It appears that the safety and feasibility of G-CSF treatment focusing on the induction of vascular occlusion in atherosclerotic lesions has not yet been established.[24] In angina patients, the administration of G-CSF was associated with the onset of acute myocardial infarction (AMI).[25] A high rate of restenosis after intracoronary infusion of G-CSF–mobilized PB-MNCs was reported in AMI patients.[16] There are articles reporting the induction of AMI and cerebral infarction in G-CSF–treated BM transplantation patients.[26,27] Differentiation of G-CSF–mobilized progenitor cells into smooth muscle cells within the stented segment as well as the induction of angiogenesis within the atherosclerotic lesion and the aggregation of mobilized inflammatory cells within the plaque may be a plausible explanation.[24] Furthermore, G-SCF–mobilized neutrophils may cause EC damage by superoxide production.[28–30] We have previously shown that polymorphonuclear cells inhibited the ischemia-induced recovery of blood perfusion in the hindlimb ischemia model.[31] Furthermore, G-CSF induces the expression of adhesion molecules on ECs, leading to leukocyte adhesion and its activation[32] or to a hypercoagulability state.[33] Thus, because G-CSF induces non-EPC populations, including neutrophil or smooth muscle progenitor cells, the enrichment of the EPC population and their application are required to inhibit such harmful effects. Indeed, the injection of G-CSF–induced circulating CD34+EPCs into ischemic limb muscle resulted in satisfactory clinical improvement.[34] Transplantation of an enriched CD34+MNC population re-established endothelial integrity in injured vessels, thereby inhibiting neointimal hyperplasia.[4] We here described that a small number (5×10^4) of enriched population c-Kit+/Flk-1+ or CD45-/Flk-1+ EPCs regenerated endothelium much more efficiently than did a large number (1×10^6) of c-Kit+/Flk-1− or CD45-/Flk-1− cells. Consistent with our observation, in the hindlimb ischemia model of mice, merely 1×10^3 CD34+/Flk-1+ cells improved limb salvage and hemodynamic recovery better than 1×10^4 CD34+/Flk-1− cells.[35] Thus, the application of an enriched EPC population may be feasible to improve the safety and efficiency of G-CSF therapy.

Increasing evidence suggests that BM-derived EPCs home to the ischemic region for the formation of new blood vessels.[2] EPCs were reportedly derived from more differentiated CD34+ or immature CD133+ hematopoietic stem cells, as well as from mature PB-MNCs or CD14+ monocytes.[5,36] They express endothelial markers, including Flk-1, FactorVIII, and endothelial NO synthase.[2,36] Intravenous infusion of BM-derived EPCs enhanced neovascularization in vivo.[37] Application of either BM-derived or PB-derived EPCs into the infarct artery beneficially affects postinfarction remodeling.[38,39] Consistent with these previous reports, we presented the data indicating that the c-Kit+/Flk-1+ cells were actually mobilized by G-CSF administration (Figure 5A), and the infusion experiment of the sorted c-Kit+/Flk-1+ EGFP cells (mobilized by G-CSF) revealed their direct involvement in the G-CSF–promoted endothelial regeneration process in the vascular repair. Thus, the stem cells expressing the Flk-1 marker are mobilized in response to G-CSF and then exert the property as an endothelial progenitor, suggesting that c-Kit+/Flk-1+ cells are the cell type responsible for G-CSF–mediated endothelial regeneration.

In conclusion, we characterized the cell type responsible for G-CSF–mediated endothelial regeneration leading to an inhibition of neointimal hyperplasia and showed that the vascular repair was mainly attributable to the G-CSF–mobilized BM-derived cells rather than G-CSF–mediated outgrowth of resident ECs, and that the repaired artery responded well to NO-mediated vasodilatory stimulus. These findings suggest that the treatment with G-CSF might be a feasible and suitable supplement therapy for the prevention of restenosis after the revascularization procedures. Although the very recent clinical study has reported that administration of G-CSF to patients with AMI improves cardiac function without any adverse events during 6-month observation,[40] G-CSF–mediated proatherogenic effects, such as the induction of angiogenesis within the atherosclerotic lesion and the aggregation of mobilized inflammatory cells within the atheromatous plaque, are the limitation of the present study and remain to be determined. Further basic and clinical studies focusing on these issues will be required.

Acknowledgments

This work was supported in part by a grant from the Ministry of Education, Culture, Science and Technology of Japan. We appreciate Dr Takeshi Todo for his great help in BM replacement experiment.

References

1. Libby P, Schwartz D, Brogi E, Tanaka H, Clinton SK. A cascade model for restenosis. A special case of atherosclerosis progression. *Circulation.* 1992;86:III47–III52..
2. Asahara T, Murohara T, Sullivan A, Silver M, van der Zee R, Li T, Witzenbichler B, Schatteman G, Isner JM. Isolation of putative progenitor endothelial cells for angiogenesis. *Science.* 1997;275:964–967.
3. Asahara T, Masuda H, Takahashi T, Kalka C, Pastore C, Silver M, Kearne M, Magner M, Isner JM. Bone marrow origin of endothelial progenitor cells responsible for postnatal vasculogenesis in physiological and pathological neovascularization. *Circ Res.* 1999;85:221–228.
4. Griese DP, Ehsan A, Melo LG, Kong D, Zhang L, Mann MJ, Pratt RE, Mulligan RC, Dzau VJ. Isolation and transplantation of autologous circulating endothelial cells into denuded vessels and prosthetic grafts: implications for cell-based vascular therapy. *Circulation.* 2003;108:2710–2715.
5. Fujiyama S, Amano K, Uchira K, Yoshida M, Nishiwaki Y, Nozawa Y, Jin D, Takai S, Miyazaki M, Egashira K, Imada T, Iwasaka T, Matsubara H. Bone marrow monocyte lineage cells adhere on injured endothelium in a monocyte chemoattractant protein-1-dependent manner and accelerate reendothelialization as endothelial progenitor cells. *Circ Res.* 2003;93:980–989.
6. Werner N, Junk S, Laufs U, Link A, Walenta K, Bohm M, Nickenig G. Intravenous transfusion of endothelial progenitor cells reduces neointima formation after vascular injury. *Circ Res.* 2003;93:e17–24.
7. Gulati R, Jevremovic D, Peterson TE, Witt TA, Kleppe LS, Mueske CS, Lerman A, Vile RG, Simari RD. Autologous culture-modified mononuclear cells confer vascular protection after arterial injury. *Circulation.* 2003;108:1520–1526.
8. Lapidot T, Petit I. Current understanding of stem cell mobilization: the roles of chemokines, proteolytic enzymes, adhesion molecules, cytokines, and stromal cells. *Exp Hematol.* 2002;30:973–981
9. Takahashi T, Kalka C, Masuda H, Chen D, Silver M, Kearney M, Magner M, Isner JM, Asahara T. Ischemia- and cytokine-induced mobilization of bone marrow-derived endothelial progenitor cells for neovascularization. *Nat Med.* 1999;5:434–438.
10. Kocher AA, Schuster MD, Szabolcs MJ, Takuma S, Burkhoff D, Wang J, Homma S, Edwards NM, Itescu S. Neovascularization of ischemic

myocardium by human bone-marrow-derived angioblasts prevents cardiomyocyte apoptosis, reduces remodeling and improves cardiac function. *Nat Med.* 2001;7:430–436.
11. Shyu WC, Lin SZ, Yang HI, Tzeng YS, Pang CY, Yen PS, Li H. Functional recovery of stroke rats induced by granulocyte colony-stimulating factor-stimulated stem cells. *Circulation.* 2004;110: 1847–1854.
12. Cotter M, Gulmann C, Jeffers M, Smith OP. Increased bone marrow angiogenesis in children with severe chronic neutropenia treated with granulocyte colony-stimulating factor. *J Pediatr Hematol Oncol.* 2004; 26:504–506.
13. Minamino K, Adachi Y, Okigaki M, Ito H, Togawa Y, Fujita K, Tomita M, Suzuki Y, Zhang Y, Iwasaki M, Nakano K, Koike Y, Matsubara H, Iwasaka T, Matsumura M, Ikehara S. Macrophage colony-stimulating factor (M-CSF), as well as granulocyte colony-stimulating factor (G-CSF), accelerates neovascularization. *Stem Cells.* 2005;23:347–354.
14. Bhattacharya V, Shi Q, Ishida A, Sauvage LR, Hammond WP, Wu MH. Administration of granulocyte colony-stimulating factor enhances endothelialization and microvessel formation in small caliber synthetic vascular grafts. *J Vasc Surg.* 2000;32:116–123.
15. Shi Q, Bhattacharya V, Hong-De Wu M, Sauvage LR. Utilizing granulocyte colony-stimulating factor to enhance vascular graft endothelialization from circulating blood cells. *Ann Vasc Surg.* 2002;16:314–320.
16. Kang HJ, Kim HS, Zhang SY, Park KW, Cho HJ, Koo BK, Kim YJ, Soo Lee D, Sohn DW, Han KS, Oh BH, Lee MM, Park YB. Effects of intracoronary infusion of peripheral blood stem-cells mobilised with granulocyte-colony stimulating factor on left ventricular systolic function and restenosis after coronary stenting in myocardial infarction: the MAGIC cell randomised clinical trial. *Lancet.* 2004;363:751–756.
17. Kong D, Melo LG, Mangi AA, Zhang L, Lopez-Ilasaca M, Perrella MA, Liew CC, Pratt RE, Dzau VJ. Cytokine-induced mobilization of circulating endothelial progenitor cells enhances repair of injured arteries. *Circulation.* 2004;110:2039–2046.
18. Okabe M, Ikawa M, Kominami K, Nakanishi T, Nishimune Y. 'Green mice' as a source of ubiquitous green cells. *FEBS Lett.* 1997;407: 313–319.
19. Minatoguchi S, Takemura G, Chen XH, Wang N, Uno Y, Koda M, Arai M, Misao Y, Lu C, Suzuki K, Goto K, Komada A, Takahashi T, Kosai K, Fujiwara T, Fujiwara H. Acceleration of the healing process and myocardial regeneration may be important as a mechanism of improvement of cardiac function and remodeling by postinfarction granulocyte colony–stimulating factor treatment. *Circulation.* 2004;109:2572–2580.
20. Chen X, Kelemen SE, Autieri MV. Expression of granulocyte colony-stimulating factor is induced in injured rat carotid arteries and mediates vascular smooth muscle cell migration. *Am J Physiol Cell Physiol.* 2005; 288:C81–C88.
21. Bussolino F, Ziche M, Wang JM, Alessi D, Morbidelli L, Cremona O, Bosia A, Marchisio PC, Mantovani A. In vitro and in vivo activation of endothelial cells by colony-stimulating factors. *J Clin Invest.* 1991;87: 986–995.
22. Sudo Y, Shimazaki C, Ashihara E, Kikuta T, Hirai H, Sumikuma T, Yamagata N, Goto H, Inaba T, Fujita N, Nakagawa M. Synergistic effect of FLT-3 ligand on the granulocyte colony-stimulating factor-induced mobilization of hematopoietic stem cells and progenitor cells into blood in mice. *Blood.* 1997;89:3186–3191.
23. Powell TM, Paul JD, Hill JM, Thompson M, Benjamin M, Rodrigo M, McCoy JP, Read EJ, Khuu HM, Leitman SF, Finkel T, Cannon RO III. Granulocyte colony-stimulating factor mobilizes functional endothelial progenitor cells in patients with coronary artery disease. *Arterioscler Thromb Vasc Biol.* 2005;25: 296–301.
24. Matsuabara H. Risk to the coronary arteries of intracoronary stem cell infusion and G-CSF cytokine therapy. *Lancet.* 2004;363:746–747.
25. Hill JM, Syed MA, Arai AE, Powell TM, Paul JD, Zalos G, Read EJ, Khuu HM, Leitman SF, Horne M, Csako G, Dunbar CE, Waclawiw MA, Cannon RO III. Outcomes and risks of granulocyte colony-stimulating factor in patients with coronary artery disease. *J Am Coll Cardiol.* 2005;46: 1643–8.
26. Kawachi Y, Watanabe A, Uchida T, Yoshizawa K, Kurooka N, Setsu K. Acute arterial thrombosis due to platelet aggregation in a patient receiving granulocyte colony-stimulating factor. *Br J Haematol.* 1996;94:413–416.
27. Fukumoto Y, Miyamoto T, Okamura T, Gondo H, Iwasaki H, Horiuchi T, Yoshizawa S, Inaba S, Harada M, Niho Y. Angina pectoris occuring during granulocyte colony-stimulating factor-combined preparatory regimen for autologous peripheral blood stem cell transplantation in a patient with acute myelogenous leukemia. *Br J Haematol.* 1997;97: 666–668.
28. Hierholzer C, Kelly E, Lyons V, Roedling E, Davies P, Billiar TR, Tweardy DJ. G-CSF instillation into rat lungs mediates neutrophil recruitment, pulmonary edema, and hypoxia. *J Leukoc Biol.* 1998;63: 169–174.
29. Azoulay E, Attalah H, Yang K, Jouault H, Schlemmer B, Brun-Buisson C, Brochard L, Harf A, Delclaux C. Exacerbation by granulocyte colony-stimulating factor of prior acute lung injury: implication of neutrophils. *Crit Care Med.* 2002;30:2115–2122.
30. Hardy MM, Flickinger AG, Riley DP, Weiss RH, Ryan US. Superoxide dismutase mimetics inhibit neutrophil-mediated human aortic endothelial cell injury in vitro. *J Biol Chem.* 1994;269:18535–18540.
31. Iba O, Matsubara H, Nozawa Y, Fujiyama S, Amano K, Mori Y, Kojima H, Iwasaka T. Angiogenesis by implantation of peripheral blood mononuclear cells and platelets into ischemic limbs. *Circulation.* 2002;8;106: 2019–2025.
32. Fuste B, Mazzara R, Escolar G, Merino A, Ordinas A, Diaz-Ricart M. Granulocyte colony-stimulating factor increases expression of adhesion receptors on endothelial cells through activation of p38 MAPK. *Haematologica.* 2004;89:578–585.
33. Canales MA, Arrieta R, Gomez-Rioja R, Diez J, Jimenez-Yuste V, Hernandez-Navarro F. Induction of a hypercoagulability state and endothelial cell activation by granulocyte colony-stimulating factor in peripheral blood stem cell donors. *J Hematother Stem Cell Res.* 2002;11: 675–681.
34. Kudo FA, Nishibe T, Nishibe M, Yasuda K. Autologous transplantation of peripheral blood endothelial progenitor cells (CD34+) for therapeutic angiogenesis in patients with critical limb ischemia. *Int Angiol.* 2003;22: 344–348.
35. Madeddu P, Emanueli C, Pelosi E, Salis MB, Cerio AM, Bonanno G, Patti M, Stassi G, Condorelli G, Peschle C. Transplantation of low dose CD34+KDR+ cells promotes vascular and muscular regeneration in ischemic limbs. *FASEB J.* 2004;18:1737–1739.
36. Urbich C, Dimmeler S. Endothelial progenitor cells: characterization and role in vascular biology. *Circ Res.* 2004;95:343–353.
37. Shintani S, Murohara T, Ikeda H, Ueno T, Sasaki K, Duan J, Imaizumi T. Augmentation of postnatal neovascularization with autologous bone marrow transplantation. *Circulation.* 2001;103:897–903.
38. Strauer BE, Brehm M, Zeus T, Kostering M, Hernandez A, Sorg RV, Kogler G, Wernet P. Repair of infarcted myocardium by autologous intracoronary mononuclear bone marrow cell transplantation in humans. *Circulation.* 2002;106:1913–1918.
39. Assmus B, Schachinger V, Teupe C, Britten M, Lehmann R, Dobert N, Grunwald F, Aicher A, Urbich C, Martin H, Hoelzer D, Dimmeler S, Zeiher AM Transplantation of Progenitor Cells and Regeneration Enhancement in Acute Myocardial Infarction (TOPCARE-AMI). *Circulation.* 2002;106:3009–3017.
40. Valgimigli M, Rigolin GM, Cittanti C, Malagutti P, Curello S, Castoldi G, Ferrari R. Use of granulocyte-colony stimulating factor during acute myocardial infarction to enhance bone marrow stem cell mobilization in humans: clinical and angiographic safety profile. *Eur Heart J.* 2005;26: 1838–1845.

Arteriosclerosis, Thrombosis, and Vascular Biology

JOURNAL OF THE AMERICAN HEART ASSOCIATION

Targeted Delivery of Bone Marrow Mononuclear Cells by Ultrasound Destruction of Microbubbles Induces Both Angiogenesis and Arteriogenesis Response

Takanobu Imada, Tetsuya Tatsumi, Yasukiyo Mori, Takashi Nishiue, Masayuki Yoshida, Hiroya Masaki, Mitsuhiko Okigaki, Hiroyuki Kojima, Yoshihisa Nozawa, Yasunobu Nishiwaki, Noriko Nitta, Toshiji Iwasaka and Hiroaki Matsubara

Arterioscler. Thromb. Vasc. Biol. 2005;25;2128-2134; originally published online Jul 28, 2005;
DOI: 10.1161/01.ATV.0000179768.06206.cb
Arteriosclerosis, Thrombosis, and Vascular Biology is published by the American Heart Association. 7272 Greenville Avenue, Dallas, TX 72514
 Print ISSN: 1079-5642. Online ISSN: 1524-4636

Targeted Delivery of Bone Marrow Mononuclear Cells by Ultrasound Destruction of Microbubbles Induces Both Angiogenesis and Arteriogenesis Response

Takanobu Imada, Tetsuya Tatsumi, Yasukiyo Mori, Takashi Nishiue, Masayuki Yoshida, Hiroya Masaki, Mitsuhiko Okigaki, Hiroyuki Kojima, Yoshihisa Nozawa, Yasunobu Nishiwaki, Noriko Nitta, Toshiji Iwasaka, Hiroaki Matsubara

Objective—Ultrasound (US)-mediated destruction of contrast microbubbles causes capillary rupturing that stimulates arteriogenesis, whereas intramuscular implantation (im) of bone marrow mononuclear cells (BM-MNCs) induces angiogenesis. We therefore studied whether US-targeted microbubble destruction combined with transplantation of BM-MNCs can enhance blood flow restoration by stimulating both angiogenesis and arteriogenesis.

Methods and Results—US-mediated destruction of phospholipid-coated microbubbles was applied onto ischemic hindlimb muscle and subsequently BM-MNCs were transfused. A significant enhancement in blood flow recovery after Bubble+US+BM-MNC infusion (34% increase, $P<0.05$) was observed compared with Bubble+US (25%). The ratio of capillary/muscle fiber increased by Bubble+US+BM-MNC-i.v (260%, $P<0.01$) than that in the Bubble+US group (172%), into which BM-MNCs were incorporated (angiogenesis). Smooth muscle α-actin–positive arterioles were also increased, and angiography showed augmented collateral vessel formation (arteriogenesis). Platelet-derived proinflammatory factors activated by Bubble+US induces the expression of adhesion molecules (P-selectin and ICAM-1), leading to the attachment of transplanted BM-MNCs on the endothelium. Flow assay confirmed that the platelet-derived factors cause the adhesion of BM-MNCs onto endothelium under laminar flow.

Conclusions—This study demonstrates that the targeted delivery of BM-MNCs by US destruction of microbubbles enhances regional angiogenesis and arteriogenesis response, in which the release of platelet-derived proinflammatory factors activated by Bubble+US play a key role in the attachment of transplanted BM-MNCs onto the endothelial layer. (***Arterioscler Thromb Vasc Biol.* 2005;25:2128-2134.**)

Key Words: angiogenesis ■ vasculogenesis ■ stem cell ■ endothelial progenitor cell ■ ultrasound

Therapeutic angiogenesis, the ability to induce the formation of new blood vessels, is one of the most promising targets for regeneration therapy. To induce angiogenesis, investigators have delivered vascular endothelial growth factor (VEGF), basic fibroblast growth factor (bFGF/FGF2). or hypoxia-inducible factor-1α/etoposide as recombinant proteins or genes.[1] Intramuscular injection of bone marrow mononuclear cells (BM-MNCs) was shown to be feasible in patients or animals with ischemic limbs by supplying angiogenic factors and endothelial progenitors.[2–4] A noninvasive cell delivery system that can target vascular endothelium would be a great advantage for manipulation of angiogenic cell therapy.

Ultrasound (US)-targeted microbubble destruction has been investigated as a new method for delivering drugs and genes to specific tissues.[5–11] This method involves the attachment of drugs or genes to gas-filled microbubbles, which are then circulated through the intravascular space and mechanically destroyed within the target organ. Theoretically, one can target any anatomic site that is accessible by US, including selected damaged regions.[5–11] Song et al have reported that US-targeted microbubble destruction causes capillary rupturing that stimulates arteriogenesis and an increase in blood flow in both normal[12] and ischemic[13] skeletal muscles, in which angiogenesis response is transient and unlikely contributes to chronic restoration of blood flow. We previously demonstrated that the recruitment of BM-MNCs and platelets stimulates angiogenesis response in ischemic muscles by releasing potent angiogenic factors, such as VEGF or bFGF, and supply of endothelial progenitors.[3,14] Furthermore, we have recently reported that systemically

Original received December 27, 2004; final version accepted May 18, 2005.

From the Department of Medicine II (T. Imada, Y.M., T.N., H. Masaki, T. Iwasaka) and Radiology (H.K.), Kansai Medical University, Osaka; the Department of Cardiovascular Medicine (T.T., M.O., H. Matsubara), Kyoto Prefectural University School of Medicine, Kyoto; the Department of Medical Biochemistry (M.Y., Y. Nishiwaki, N.N.), Graduate School of Medicine, Tokyo Medical and Dental University, Tokyo; and the Pharmacobioregulation Research Laboratory (Y. Nozawa), Taiho Pharmaceutical Co Ltd, Saitama, Japan.

T. Iwasaka and H. Matsubara contributed equally to this study.

Correspondence to Hiroaki Matsubara MD, Department of Cardiovascular Medicine, Kyoto Prefectural University School of Medicine, Kamigyo-ku, Kyoto, 602-8566, Japan. E-mail matsubah@koto.kpu-m.ac.jp

Arterioscler Thromb Vasc Biol. **is available at http://www.atvbaha.org** **DOI: 10.1161/01.ATV.0000179768.06206.cb**

transplanted BM-MNCs can be firmly attached onto the injured vascular endothelium in an adhesive molecule–dependent manner.[15] We therefore examined whether US-targeted microbubble destruction combined with intravenous transplantation of BM-MNCs causes angiogenesis response as well as arteriogenesis in a rat model with an ischemic hindlimb, leading to an enhancement of chronic blood flow restoration. Interestingly, we found that platelet-derived factors activated by US-targeted microbubble destruction induce the expression of adhesive molecules on the endothelium and subsequent attachment of transplanted BM-MNCs, resulting in an enhancement of formation of neocapillaries and new arterioles and an increase in regional blood flow recovery.

Materials and Methods

Microbubble Preparations

BR14 (Bracco Diagnostics) is a new ultrasound contrast agent, consisting of perfluorocarbon-containing microbubbles stabilized by a phospholipid monolayer.[16,17] The suspension of gas microbubbles is reconstituted immediately before use by injecting 5 mL of 0.9% sodium chloride. The mean diameter of bubbles is 2.3 to 2.5 μm and the bubble concentration is $\approx 6\times10^8$ per ml. BR14 was administered as a 1 mL bolus injection via contralateral femoral vein.

Isolation of BM-MNC and Characterization of Endothelial-Lineage Cells

BM-MNCs were isolated from SEA/LEW rat femoral bone and centrifuged by density gradient (Lymphoprep; Nycomed). The MNC fraction was labeled with red-fluorescence cell linker (PKH26-GL; Sigma).[2,3,14] Endothelial lineage cells were analyzed by fluorescence-activated cell sorter (FACS) using DiI-acetylated LDL (acLDL) incorporation (Biogenesis) and Ulex lectin binding (Sigma) as described previously.[2,3,14]

Hindlimb Ischemia, US Application, and Transfusion of BM-MNCs

Unilateral hindlimb ischemia was induced by resecting the left femoral artery as described.[2,18] Arteriogenesis that restores the regional blood flow was reported to be observed 3 days after induction of limb ischemia of rats.[12,13] We therefore performed the infusion of microbubble at day 3 after limb ischemia to efficiently deliver microbubble BR14 to the ischemic site. We divided the rats into the following five groups: (1) Control (saline injection, n=8); (2) Bubble (1 mL BR14)+US (n=8); (3) Bubble+US+BM-MNC-i.v. (n=8), BM-MNC (2×10^7 in 1 mL saline) injected from contralateral femoral vein 1 minute after Bubble+US; (4) BM-MNC-i.m. (n=8), BM-MNC (2×10^7) intramuscularly implanted into the ischemic limb; and (5) BM-MNC-i.v. (n=8); BM-MNC (2×10^7 in 1 mL saline). BM-MNC (2×10^7) included $0.3\pm0.04\times10^7$ platelets.

The skin overlying the ischemic thigh muscle to be treated was reflected back, ultrasound gel was placed over the ischemic muscle, and 1-MHz transducer (S-probe, Effective Radiating Area: 0.9 cm^2; Ito Co Ltd) was held 3 mm over the muscle and to keep the skin temperature around $\approx$37°C. A continuous sinusoidal wave ultrasound (1MHz, 2W/cm^2, Beam Nonuniformity Ratio: 3.6; ITO-US-700) was applied for 1 minute immediately after microbubble injection. To clarify whether the microbubbles really reach ischemic tissues after infusion from contralateral femoral vein, the delivery of injected microbubbles to the ischemic area was examined by a diagnostic ultrasound echography (Sonos-5500) equipped with an ultraband S12 sector transducer.

Evaluation of Neocapillary and Immunohistochemical Analysis

Four pieces of ischemic tissues from the adductor and semimembranous muscles were obtained 28 days after limb ischemia. Frozen sections were stained with antibodies for smooth muscle (SM) α-actin (Sigma) and anti-factor VIII (DAKO) antibodies. The appropriate secondary antibodies conjugated with fluorescein isothiocyanate (FITC) or rhodamine were used. Ten fields from 2 muscle samples of each animal were randomly selected for the vessel count. To ensure that vessel densities were not overestimated as a consequence of myocyte atrophy or underestimated because of interstitial edema, the capillary/muscle fiber ratio was determined.[3,18]

Electron Microscope

Femoral arteries in skeletal muscles on which targeted US was applied were isolated after Bubble+US treatment (n=4), fixed by 2.5% glutaraldehyde and 1.5% osmium acid, dried, and viewed by electron microscope (HITATI S-700).[15]

Cell Culture and Platelet-Rich Plasma Isolation

Human umbilical vein endothelial cells (HUVECs; Kurabo) were cultured in HuMedia-EG2 medium. For use in the study apparatus, HUVECs (2nd or 3rd passages) were plated on 22-mm fibronectin-coated cover slips.[15] Peripheral blood was drawn from healthy volunteers and mixed with 0.1 volume of citrate (108 mmol/L). Whole blood was centrifuged at 150g for 10 minutes to harvest platelet-rich plasma (PRP).

Adhesion Assay Under Laminar Flow and Immunofluorescence Study

HUVECs were incubated for 30 minutes with serum-free medium with or without freshly prepared 10% platelet-rich plasma, and then stimulated by (1) 10% Bubble+US (1MHz, 1.5W, 30 seconds) in 10% PRP (Bubble+US with platelet group), (2) 10% Bubble+US in PRP (Bubble+US without platelet), (3) incubation media (in which 10% platelet-rich medium was stimulated by 10% Bubble+US), or (4) US with platelet (in which 10% platelet-rich medium was stimulated by US alone), n=6 in each experiment. HUVECs were placed on the cold plate to prevent the heating by the US, and adhesion assay under laminar flow was performed as previously described.[15] For further detail, please see the supplemental Methods, available online at http://atvb.ahajournals.org.

Stimulated HUVECs were fixed by 4% paraformaldehyde 1 hour after stimulation and incubated with anti–P-selectin (R&D Systems, Inc) and anti-platelet glycoprotein (GP)-Ib antibody (DAKO). The appropriate secondary antibodies conjugated with FITC or rhodamine were used. Nuclei were stained with 4′,6′-diamidino-2-phenylindole dihydrochloride (DAPI) and viewed by a fluorescence microscope (Olympus OX71).

Laser Doppler Perfusion Image and Angiography

Laser doppler perfusion image (LDPI) and angiography were performed as previously described[3,18] For further detail, please see the supplemental Methods.

Statistical Analysis

Statistical analyses were performed with 1-way ANOVA followed by pair-wise contrasts using the Dunnett test. Data (mean±SE) were considered statistically significant when $P<0.05$.

Results

Incidence of Endothelial-Lineage Cells in BM-MNCs

FACS analysis indicated that 28±1.8% and 31±1.5% of BM-MNCs incorporated DiI-acLDL and bound Ulex-lectin (n=5), respectively, and 20±1.2% of cells were positive for both markers. Endothelial-lineage cells were considered to be included in this fraction as reported.[2,3,14]

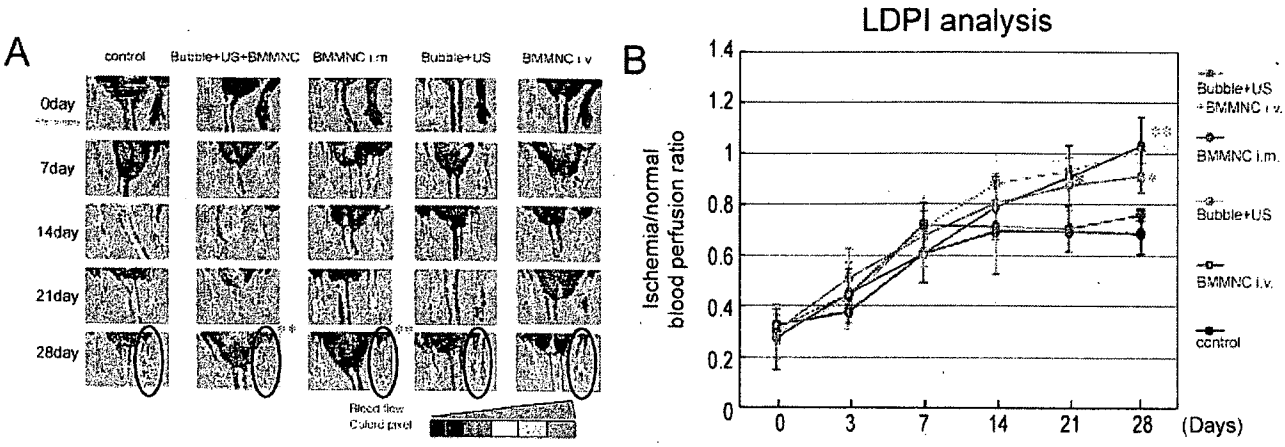

Figure 1. Increase of blood flow by US-microbubble-mediated transfusion of BM-MNCs. A, Representative LDPI. Greater blood perfusion (red to yellow) in ischemic limbs was observed in Bubble+US+BM-MNC infusion, BM-MNC-i.m., and Bubble+US groups in contrast with the untreated control and BM-MNC-i.v. groups. B, Computer-assisted analyses of LDPI revealed a significantly greater blood perfusion in the Bubble+US+BM-MNC-i.v., BM-MNC-i.m., and Bubble+US groups than in the control group. The values shown are mean±SE (n=8) at each time point. *$P<0.05$, **$P<0.01$ vs control.

Laser Doppler Blood Perfusion

Subcutaneous blood perfusion was analyzed by LDPI imaging (Figure 1). Intravenous injection of BM-MNCs (BM-MNC-i.v.) did not cause a significant increase in the blood flow recover compared with the control (saline injection; Figure 1). Treatment with Bubble+US without BM-MNCs-i.v. showed a moderate increase (25±2% at Day 28 versus control, $P<0.05$), whereas the combination of Bubble+US and BM-MNCs-i.v. induced a further increase (34±2% versus control at Day 28, $P<0.01$), which was significantly higher than that of Bubble+US manipulation alone ($P<0.05$). The blood perfusion recovery by Bubble+US+BM-MNC-i.v. was comparable to blood perfusion by BM-MNC-i.m. (38±3%). Blood perfusion after US+BM-MNC-i.v. without Bubble did not significantly differ from those in BM-MNC-i.v. alone or control groups (3±1% versus control at Day 28, n=8; data not shown), suggesting that the combination of BM-MNCs infusion with Bubble+US significantly improves the blood flow recovery after limb ischemia compared with each manipulation alone, and that the efficient cell delivery system depends on US-mediated destruction of microbubbles.

Neocapillary and Arteriole Formation

Formation of capillaries and arterioles was evaluated by factor VIII–positive and SM α-actin–positive vessels. The ratio of capillary/muscle fiber (factor VIII–positive and SM α-actin–negative vessel) was significantly increased in the Bubble+US+BM-MNC-i.v. group (260±15% versus control, $P<0.01$), which was greater ($P<0.01$) than that of Bubble+US group (172±11% versus control, $P<0.05$). The ratio of arteriole/muscle fiber (factor VIII–positive and SM α-actin–positive vessel) was also increased by Bubble+US+BM-MNC-i.v. (188±10% versus control, $P<0.01$), which was greater ($P<0.05$) than that in the Bubble+US group (146±9% versus control, $P<0.05$; Figure 2A). Transfused BM-MNCs (labeled with red fluorescence) were found to be incorporated into microvessels by Bubble+US+BM-MNC-i.v. (arrows in Figure 2B). These findings suggest that Bubble+US+BM-MNC-i.v. enhances both angiogenesis as well as arteriogenesis response.

To examine the specificity of this cell delivery system, we examined the distribution of transfused BM-MNCs in other tissues (kidney, spleen, liver, heart, pancreas, small intestines, and brain) 3 weeks after targeted cell delivery by Bubble+US+BM-MNCs-iv. Small numbers of labeled BM-MNCs were detected in the kidney (mainly in the tubule) and greater numbers of BM-MNCs were observed in the spleen, whereas no labeled cells were detected in other tissues (Figure I, available online at http://atvb.ahajournals.org).

Arteriogenesis Response Evaluated by Angiography

Compared with angiogenesis formed by capillary sprouting, arteriogenesis is often studied with the use of angiography. On the postoperative day 28, all animals were subjected to iliac angiography. Representative angiograms (n=4 in each group) are shown in Figure II (available online at http://atvb.ahajournals.org), in which arrows indicate the ligated ends of femoral arteries. Collateral vessels in the thigh area were quantitatively counted using 5-mm^2 grids.[3,18] An apparent increase in collateral vessel formation was observed in the Bubble+US+BM-MNC-i.v. and BM-MNC-i.m. (4.2±0.2-fold and 4.3±0.2-fold, n=6, respectively; $P<0.001$) compared with that in the BM-MNC-i.v. group. The increase in the Bubble+US group was 1.8±0.1-fold ($P<0.05$) when compared with that in the BM-MNC-i.v. group, which was significantly smaller ($P<0.01$) than that of the Bubble+US+BM-MNC-i.v. group. There was no significant difference between control (saline infusion) and BM-MNC-i.v. groups.

Delivery of Microbubbles to the Ischemic Muscle

Arteriogenesis that restores the regional blood flow was observed 3 days after induction of limb ischemia of rats.[12,13] We therefore performed the infusion of microbubble at day 3 after limb ischemia to efficiently deliver microbubble BR14

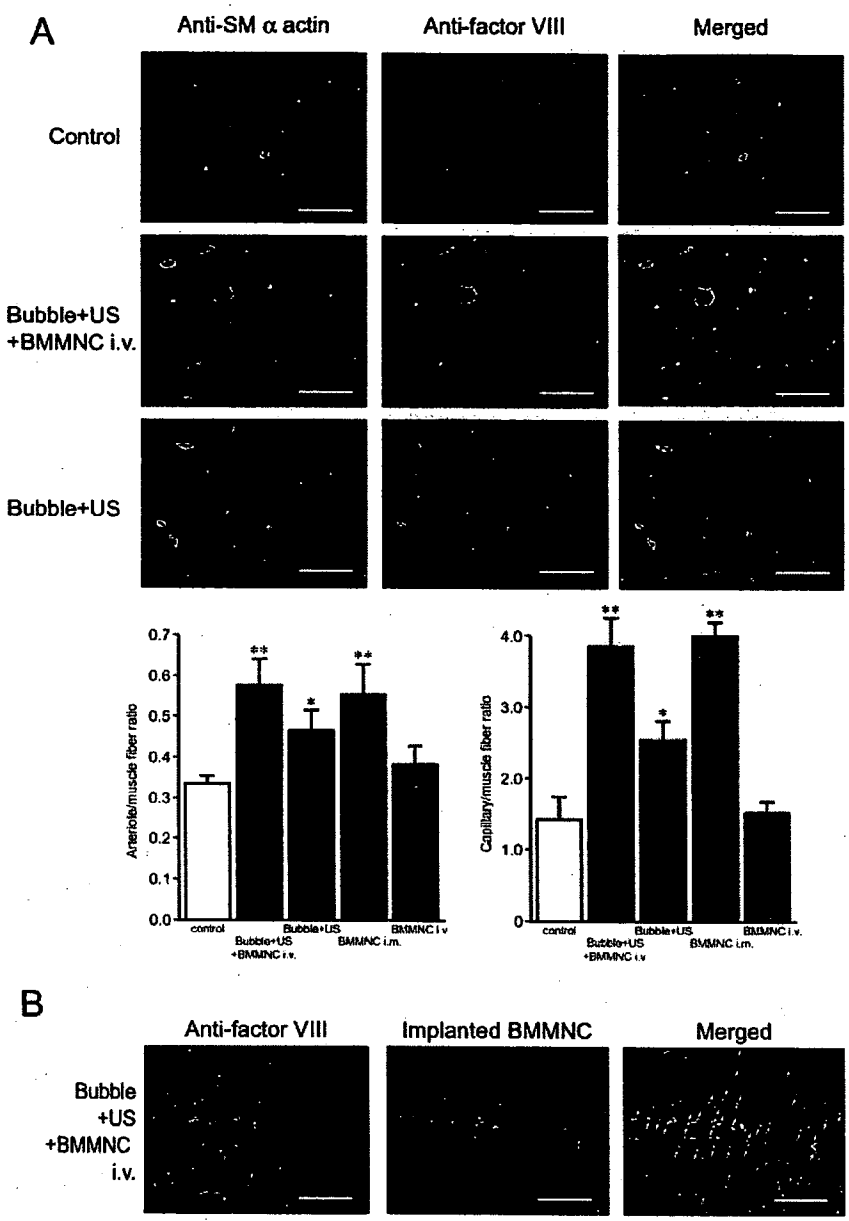

Figure 2. Formation of arterioles/capillaries and incorporation of transfused BM-MNCs. A, Vessels were immunostained with anti-SM α-actin and anti-factor VIII antibodies. Numbers for arterioles (positive for both SM α-actin and factor VIII staining) and capillaries (SM α-actin–negative and factor VIII–positive) were evaluated as a vessel number/muscle fiber ratio (n=8, each group). $^{*}P<0.05$, $^{**}P<0.01$ vs the saline-injected control. Bar=50 μm. B, Incorporation of transfused BM-MNCs (labeled with red-fluorescence). Red-labeled cells were incorporated into factor VIII–positive capillaries (arrows in the merged image) in the Bubble+US+BM-MNC-i.v. group. Data shown are representative of 5 different animals. Bar=200 μm.

to the ischemic site. We further examined whether the transfused microbubbles really reach the hindlimb muscle at 3 days after induction of ischemia. Apparent increase in the contrast densities in the ischemic thigh muscle (indicated by arrows in Figure III, available online at http://atvb.ahajournals.org) was observed ≈15 seconds after injection of microbubbles in both control (normal) and ischemic limbs compared with the pre-images before injection of microbubbles. The increase in contrast shadow diminished after 1 minute of US stimulation, indicating that microbubbles really reach ischemic hindlimb muscles after venous infusion.

Electromicroscopy

A previous study reported the presence of small holes in the endothelial cells treated with Bubble+US,[11] whereas we could not detect the presence of apparent small holes in the vascular endothelium in the skeletal muscle on which the Bubble+US was applied. Neither adhesion of MNCs nor formation of fibrin network including platelets was detected on the surface of normal endothelium or endothelium stimulated by US without microbubbles. Interestingly, we found the attachment of platelets associated with fibrin network and MNCs on the surface of endothelium in all arteries treated by Bubble+US+BM-MNCs infusion (n=6; Figure 3), whereas no adhesion of platelets or MNCs was detected in the US+BM-MNC group without microbubbles (n=6; data not shown).

Induction of Adhesion Molecules

We have reported that transplanted BM-MNCs can firmly attach onto the injured vascular endothelium in an adhesive molecule–dependent manner.[15] We therefore examined the expression profile of adhesive molecules on HUVECs treated by Bubble+US. The expression of adhesive molecules (P-selectin or ICAM-1) was not induced when HUVECs were